



# **NAVAL POSTGRADUATE SCHOOL**

**MONTEREY, CALIFORNIA**

## **THESIS**

**ACOUSTIC CYMBAL TRANSDUCERS – DESIGN,  
HYDROSTATIC PRESSURE COMPENSATION, AND  
ACOUSTIC PERFORMANCE**

by

Kirk E. Jenne

March 2004

Thesis Advisor:  
Thesis Co-Advisor:

Thomas R. Howarth  
Dehua Huang

**Approved for public release; distribution unlimited**

THIS PAGE INTENTIONALLY LEFT BLANK

<b>REPORT DOCUMENTATION PAGE</b>			Form Approved OMB No. 0704-0188	
Public reporting burden for this collection of information is estimated to average 1 hour per response, including the time for reviewing instruction, searching existing data sources, gathering and maintaining the data needed, and completing and reviewing the collection of information. Send comments regarding this burden estimate or any other aspect of this collection of information, including suggestions for reducing this burden, to Washington headquarters Services, Directorate for Information Operations and Reports, 1215 Jefferson Davis Highway, Suite 1204, Arlington, VA 22202-4302, and to the Office of Management and Budget, Paperwork Reduction Project (0704-0188) Washington DC 20503.				
<b>1. AGENCY USE ONLY (Leave blank)</b>		<b>2. REPORT DATE</b> March 2004	<b>3. REPORT TYPE AND DATES COVERED</b> Master's Thesis	
<b>4. TITLE AND SUBTITLE:</b> Acoustic Cymbal Transducers – Design, Pressure Compensation, and Acoustic Performance			<b>5. FUNDING NUMBERS</b>	
<b>6. AUTHOR(S)</b> Kirk E. Jenne				
<b>7. PERFORMING ORGANIZATION NAME(S) AND ADDRESS(ES)</b> Naval Postgraduate School Monterey, CA 93943-5000			<b>8. PERFORMING ORGANIZATION REPORT NUMBER</b>	
<b>9. SPONSORING /MONITORING AGENCY NAME(S) AND ADDRESS(ES)</b> Naval Undersea Warfare Center Underwater Sensors and Sonar Systems Department Newport, RI 02841-1708			<b>10. SPONSORING/MONITORING AGENCY REPORT NUMBER</b>	
<b>11. SUPPLEMENTARY NOTES</b> The views expressed in this thesis are those of the author and do not reflect the official policy or position of the Department of Defense or the U.S. Government.				
<b>12a. DISTRIBUTION / AVAILABILITY STATEMENT</b> Approved for public release; distribution is unlimited			<b>12b. DISTRIBUTION CODE</b>	
<b>13. ABSTRACT (maximum 200 words)</b>  Continuing U.S. Navy interest in the development of light-weight, low-volume, broadband, underwater acoustic projectors and receivers is the principal motivation for this research topic. Acoustic cymbal transducers, so named for their geometric similarity to the percussion instruments, are miniature “class V” flexensional transducers that consist of a piezoelectric ceramic drive element bonded to two opposing cymbal-shaped metal shells. Operating as mechanical transformers, the two metal shells convert the naturally large generative force of a piezoelectric ceramic in the radial mode into increased volume displacement at the metal shell surface to obtain usable source levels and sensitivities in a broad frequency range. The magnified displacement makes the acoustic cymbal element a potential alternative to acoustic transduction technologies presently used to generate and receive Navy sonar frequencies. Potential benefits to utilizing this technology are generating or receiving broadband sound, at sonar frequencies in a thin, low volume, conformable package. Applications of this technology have been limited because air-backed acoustic cymbal elements undergo degradation in performance when exposed to elevated hydrostatic pressure (i.e., deep ocean and extreme littoral water applications). This research shows that consistent and reliable acoustic performance can be achieved with cymbal-based transducers at hydrostatic pressures of interest to the Navy.				
<b>14. SUBJECT TERMS</b> Acoustic Calibration, Underwater Acoustics, Underwater Sound, Transducer, Flexensional, Acoustic Cymbal, Broadband, USRD, APTF, Piezoelectric, Piezoceramic, Array Elements, Hydrostatic Pressure, Pressure Compensation, Sonar			<b>15. NUMBER OF PAGES</b> 99	
			<b>16. PRICE CODE</b>	
<b>17. SECURITY CLASSIFICATION OF REPORT</b> Unclassified	<b>18. SECURITY CLASSIFICATION OF THIS PAGE</b> Unclassified	<b>19. SECURITY CLASSIFICATION OF ABSTRACT</b> Unclassified	<b>20. LIMITATION OF ABSTRACT</b> UL	

THIS PAGE INTENTIONALLY LEFT BLANK

**Approved for public release; distribution unlimited**

**ACOUSTIC CYMBAL TRANSDUCERS – DESIGN, PRESSURE  
COMPENSATION, AND ACOUSTIC PERFORMANCE**

Kirk E. Jenne  
ND04, Navy Civilian  
B.S., Florida Atlantic University, 1984

Submitted in partial fulfillment of the  
requirements for the degree of

**MASTER OF SCIENCE IN ENGINEERING ACOUSTICS**

from the

**NAVAL POSTGRADUATE SCHOOL  
March 2004**

Author: Mr. Kirk E. Jenne

Approved by: Thomas R. Howarth  
Thesis Advisor, NAVSEA Div Newport

Dehua Huang  
Thesis Co-Advisor, NAVSEA Div Newport

Thomas J. Hofler  
Thesis Co-Advisor, NPS Physics Dept

Kevin B. Smith  
Chair, Engineering Acoustics Academic Committee

THIS PAGE INTENTIONALLY LEFT BLANK

## **ABSTRACT**

Continuing U.S. Navy interest in the development of light-weight, low-volume, broadband, underwater acoustic projectors and receivers is the principal motivation for this research topic. Acoustic cymbal transducers, so named for their geometric similarity to the percussion instruments, are miniature “class V” flextensional transducers that consist of a piezoelectric ceramic drive element bonded to two opposing cymbal-shaped metal shells. Operating as mechanical transformers, the two metal shells convert the naturally large generative force of a piezoelectric ceramic in the radial mode into increased volume displacement at the metal shell surface to obtain usable source levels and sensitivities in a broad frequency range. The magnified displacement makes the acoustic cymbal element a potential alternative to acoustic transduction technologies presently used to generate and receive Navy sonar frequencies. Potential benefits to utilizing this technology are generating or receiving broadband sound, at sonar frequencies in a thin, low volume, conformable package. Applications of this technology have been limited because air-backed acoustic cymbal elements undergo degradation in performance when exposed to elevated hydrostatic pressure (i.e., deep ocean and extreme littoral water applications). This research shows that consistent and reliable acoustic performance can be achieved with cymbal-based transducers at hydrostatic pressures of interest to the Navy.

THIS PAGE INTENTIONALLY LEFT BLANK



## TABLE OF CONTENTS

<b>I.</b>	<b>UNDERWATER ELECTROACOUSTIC TRANSDUCERS .....</b>	<b>1</b>
<b>A.</b>	<b>SELECTED HISTORY .....</b>	<b>1</b>
<b>B.</b>	<b>FLEXTENSIONAL TRANSDUCERS .....</b>	<b>2</b>
1.	History of the Flextensional Transducer .....	3
2.	Mechanics of Operation .....	4
<b>C.</b>	<b>MINIATURE FLEXTENSIONAL CONCEPT .....</b>	<b>4</b>
<b>II.</b>	<b>ACOUSTIC CYMBAL ELEMENT COMPONENTS .....</b>	<b>7</b>
<b>A.</b>	<b>PIEZOELECTRIC DRIVER .....</b>	<b>7</b>
1.	Piezoelectric Effect.....	7
2.	Piezoelectric Relations and Crystallographic Structure .....	8
3.	Manufacturing of Piezoceramics .....	11
4.	Property Specifications.....	12
5.	Piezoceramic Material Types Considered .....	14
<b>B.</b>	<b>FLEXURAL SHELL .....</b>	<b>15</b>
1.	Material.....	15
2.	Flexural Shell Configuration .....	16
3.	Manufacturing.....	18
<b>C.</b>	<b>EPOXY AND BOND JOINT .....</b>	<b>19</b>
<b>III.</b>	<b>FABRICATION OF ACOUSTIC CYMBAL ELEMENTS .....</b>	<b>21</b>
<b>A.</b>	<b>FLEXURAL SHELLS .....</b>	<b>21</b>
<b>B.</b>	<b>TITANIUM STUD AND WELDMENT .....</b>	<b>21</b>
<b>C.</b>	<b>ASSEMBLING THE CYMBAL SHELL .....</b>	<b>23</b>
<b>D.</b>	<b>FINAL STAGE OF ASSEMBLY .....</b>	<b>25</b>
<b>E.</b>	<b>MOUNTING FIXTURE FOR ACOUSTIC TESTS.....</b>	<b>25</b>
<b>IV.</b>	<b>IN-AIR EVALUATION OF CYMBAL ELEMENTS.....</b>	<b>29</b>
<b>A.</b>	<b>IMPEDANCE AND ADMITTANCE .....</b>	<b>29</b>
1.	Admittance Data .....	30
<b>B.</b>	<b>SCANNING LASER VIBROMETRY .....</b>	<b>30</b>
1.	Test Equipment and Interpretation of Data.....	31
2.	SLV Measurement at 2 kHz.....	32
3.	SLV Measurements at 14 kHz .....	33
4.	SLV Measurement at 30 kHz.....	34
5.	SLV Measurement at 40 kHz.....	35
<b>V.</b>	<b>UNDERWATER ACOUSTIC MEASUREMENTS.....</b>	<b>37</b>
<b>A.</b>	<b>FREE FIELD VOLTAGE SENSITIVITY.....</b>	<b>37</b>
<b>B.</b>	<b>TRANSMITTING VOLTAGE RESPONSE.....</b>	<b>38</b>
<b>C.</b>	<b>ACOUSTIC TEST FACILITY.....</b>	<b>39</b>
<b>VI.</b>	<b>ACOUSTIC CYMBAL CONFIGURATIONS &amp; TEST RESULTS.....</b>	<b>43</b>
<b>A.</b>	<b>PRESSURE COMPENSATION FOR UNDERWATER TRANSDUCERS.....</b>	<b>43</b>
1.	Passive Pressure Compensation Systems.....	43

2.	Active Pressure Compensation Systems .....	44
3.	Pressure Testing.....	44
B.	NAVY ACOUSTIC CYMBAL ELEMENT “STANDARD” .....	45
C.	INVERTED RING SHELLS OR “DOUBLE-DIPPERS” .....	48
1.	One mm Thick Driver Element .....	49
2.	Three Millimeter Thickness .....	50
D.	CYMBAL ELEMENTS OF VARYING SHELL DEPTHS.....	52
1.	Type 600 .....	52
2.	Type 900 .....	54
E.	ACOUSTIC CYMBAL ELEMENTS WITH PORTS.....	56
1.	Holes Near the Apex (Apex Holes) .....	56
2.	Shells with Slots.....	59
3.	Small Holes at Outer Edge (Edge Holes) .....	61
F.	ACOUSTIC MEASUREMENTS SUMMARIZED .....	64
	LIST OF REFERENCES.....	67
	APPENDIX A – APTF DATA DIRECTORY 2104.....	71
	APPENDIX B – APTF DATA DIRECTORY 2169 .....	73
	APPENDIX C – APTF DATA DIRECTORY 2228.....	75
	APPENDIX D – TRANSDUCER COORDINATE SYSTEM .....	77
	INITIAL DISTRIBUTION LIST .....	79

## LIST OF FIGURES

Figure 1.	The “Fessenden Oscillator” from Ref [1]	2
Figure 2.	Underwater flextensional transducer from Ref [4]	3
Figure 3.	Representation of Perovskite structure for $\text{CaTiO}_3$ from Ref [18.5]	9
Figure 4.	Illustration of piezoelectric parameter subscripts from Ref [19]	10
Figure 5.	Resonance frequency (in-air) vs. cavity depth for various materials	16
Figure 6.	Resonance frequency (in-air) vs. cavity diameter - related to cavity depth	17
Figure 7.	Resonance frequency (in-air) vs. apex diameter - related to cavity diameter	18
Figure 8.	Resonance frequency (in-air) vs. bond line width	19
Figure 9.	Instron pull test on cymbal shell to determine strength	20
Figure 10.	Three views of titanium cymbal shells	21
Figure 11.	Two studs used for welding to center of apex	22
Figure 12.	Stud welding apparatus	23
Figure 13.	Placing stud in the collet	23
Figure 14.	Lap bonding surface of flange to remove burrs	24
Figure 15.	Epoxy coated piezoceramic is placed into assembly fixture	24
Figure 16.	Top plate being bolted into place	25
Figure 17.	Acoustic test platform for cymbal elements	26
Figure 18.	Close-up of cymbal element in acoustic test fixture	26
Figure 19.	Author installing acoustic cymbal transducers	27
Figure 20.	Admittance plot (with phase) of acoustic cymbal element	30
Figure 21.	2 kHz laser scan of cymbal shell in 3-d, contractional mode	32
Figure 22.	2 kHz laser scan of cymbal shell in 3-d, extensional mode	33
Figure 23.	14 kHz laser scan of cymbal shell in 3-d, contractional mode	34
Figure 24.	14 kHz laser scan of cymbal shell in 3-d, extensional mode	34
Figure 25.	30 kHz laser scan of cymbal shell in 3-d, contractional mode	35
Figure 26.	30 kHz laser scan of cymbal shell in 3-d, extensional mode	35
Figure 27.	40 kHz laser scan of cymbal shell in 3-d	36
Figure 28.	40 kHz laser scan of cymbal shell in 2-d	36
Figure 29.	Cross-sectional diagram of the APTF	40
Figure 30.	End view of insulcrete wedges at one end of the APTF	41
Figure 31.	Navy acoustic cymbal element ‘standard’ design	45
Figure 32.	FFVS of cymbal element standard at varying pressures (psi)	47
Figure 33.	TVR of cymbal element standard at varying pressures (psi)	47
Figure 34.	FFVS of double-dipper (1mm thick) at varying pressures (psi)	49
Figure 35.	TVR of double-dipper (1mm thick) at varying pressures (psi)	50
Figure 36.	FFVS of double-dipper (3mm thick) at varying pressures (psi)	51
Figure 37.	TVR of double-dipper (3mm thick) at varying pressures (psi)	51
Figure 38.	FFVS of cymbal element type 600 at varying pressures (psi)	53
Figure 39.	TVR of cymbal element type 600 at varying pressures (psi)	54
Figure 40.	FFVS of cymbal element type 900 at varying pressures (psi)	55
Figure 41.	TVR of cymbal element type 900 at varying pressures (psi)	55

Figure 42.	Cymbal elements with holes near the apex.....	56
Figure 43.	FFVS of cymbal element with apex holes at varying pressures (psi).....	58
Figure 44.	TVR of cymbal element with apex holes at varying pressures (psi) .....	58
Figure 45.	Cymbal element with Slots .....	59
Figure 46.	FFVS of cymbal element with slots at varying pressures (psi) .....	60
Figure 47.	TVR of cymbal element with slots at varying pressures (psi) .....	60
Figure 48.	Cymbal element with very small holes near inner edge of flange.....	61
Figure 49.	FFVS of cymbal element with edge holes at varying pressures (psi).....	63
Figure 50.	TVR of cymbal element with edge holes at varying pressures (psi) .....	63

## LIST OF TABLES

Table 1.	General Properties of Navy Piezoceramic Types .....	12
Table 2.	Vernitron Listing of Typical PZT Properties.....	13
Table 3.	Test Matrix for Cymbal Element Standards .....	46
Table 4.	Test Matrix for Double-Dipper Cymbal Elements .....	48
Table 5.	Test Matrix for Cymbal Elements of varying heights .....	52
Table 6.	Test Matrix for Cymbal Element with Holes Near Apex .....	57
Table 7.	Test Matrix for Cymbal Elements with Slots .....	59
Table 8.	Test Matrix for Cymbal Elements with Edge Holes.....	62

THIS PAGE INTENTIONALLY LEFT BLANK

## LIST OF ABBREVIATIONS, ACRONYMS, SYMBOLS

### A-C

Ag – Silver  
ATF – Acoustic Test Facility  
APTF – Acoustic Pressure Tank Facility  
AMB – Ambient (refers to pressure)  
BaTiO<sub>3</sub> – Barium Titanate  
°C – degrees Centigrade  
CaTiO<sub>3</sub> – Calcium Titanate  
CW – Clockwise  
Cu – Copper

### D-F

$d$  – distance  
 $d_{mj}$  – piezoelectric charge constant  
 $D$  – piezoelectric charge per unit area  
dB – deciBel(s)  
dc – direct current  
 $E$  – Electric Field  
 $\epsilon_0$  – permittivity of free space  
 $\epsilon_{mn}^T$  – dielectric constant of a ceramic  
 $e_{oc}$  – open circuit voltage  
 $e_s$  – open circuit voltage from a calibrated reference hydrophone  
 $e_x$  – unknown open circuit voltage from a hydrophone under test  
FFVS – Free-Field Voltage Sensitivity

### G-J

$g_{ij}$  – piezoelectric voltage constant  
 $J$  – Reciprocity parameter

### K-N

$K_{33}^T$  – Free Dielectric Constant  
kHz – kiloHertz  
kPa – kilopascal  
 $M$  – Sensitivity of a hydrophone  
 $M_s$  – Sensitivity of reference hydrophone  
 $M_x$  – Sensitivity of a hydrophone under test  
MPa – megaPascal  
MRA – Main response axis  
MRL – Materials Research Laboratory

$\mu\text{Pa}$  – microPascal  
Ni – Nickel  
NUWC – Naval Undersea Warfare Center

#### P-S

p – free-field sound pressure (in  $\mu\text{Pa}$ )  
Pa – Pascal  
 $\text{PbZrO}_3$  – Lead Zirconate Titanate  
psi – pounds per square inch  
PZT – Lead Zirconate Titanate  
R – Electrical resistance  
 $s^E_{ij}$  – material elastic modulus  
S – Transmitting Response  
SCUBA – Self-contained underwater breathing apparatus  
SLV – Scanning Laser Vibrometer (or Vibrometry)  
SST – Stainless Steel

#### T-Z

T – Mechanical Stress  
TVR – Transmitting Voltage Response  
V – Volts  
 $V_{\text{rms}}$  – Volts, root mean square  
WWI – World War I  
X – Electrical reactance  
Y – Electrical admittance  
Z – Electrical impedance



## **ACKNOWLEDGMENTS**

I offer my sincere appreciation to colleagues and advisors Dr. Thomas R. Howarth and Dr. Dehua Huang, and my supervisor Dr. Joseph F. Zalesak, from NAVSEA Newport, Dr. Thomas Hofler from the Naval Postgraduate School, and Dr. James Tressler at the Naval Research Laboratory in Washington, DC for their enthusiasm and willingness to offer technical guidance and support throughout various stages of this investigation.

The gracious support and earnest collaboration extended to me by Dr. Robert E. Newnham and Mr. Douglas Markley at The Pennsylvania State University is sincerely appreciated.

I extend my thanks to those at the Naval Surface Warfare Center at Crane for their valuable contributions; Mr. Walter Carney and Mr. Scott Small for their valuable assistance throughout the manufacturing processes, and Mr. James Merryfield for his artful assistance with rubber molding.

It was a great pleasure to work with and receive support from a dedicated measurement acoustician at the USRD Acoustic Pressure Tank Facility, my good friend and colleague Mr. Tony Paolero.

Heartfelt thanks go out to my wife, Christine Jenne, our children – Trevor, Conrad, Kierstin, and Rebekah, and my parents, Carl and Pat for the support and encouragement offered during my many hours and days away from home. To them especially, I dedicate this work.

Kirk Jenne

March 2004

THIS PAGE INTENTIONALLY LEFT BLANK

## **EXECUTIVE SUMMARY**

Acoustic cymbal technologies have shown potential and capability as underwater acoustic transduction devices. As underwater sound projectors, acoustic cymbal technology is being considered for emerging Navy applications that are being tested under controlled conditions in shallow water. To extend the capability and reduce the limiting factors for these applications, acoustic cymbal elements need to be modified to perform consistently when exposed to deep-ocean and extreme littoral waters.

Transduction technologies that free up underwater interior volumes now occupied by large sonar elements are of great interest to the Navy. There are many benefits to increasing bandwidth not achievable by specific highly resonant, large volume transducers that have been traditionally used in U.S. Navy sonar systems. Increased bandwidth allows for multiple functions as well as advanced capabilities within the same sonar suite. Thin, planar and curved arrays featuring multiple acoustic cymbal elements have already shown potential for broadband performance from below 1 kHz to greater than 100 kHz.

The intent of this research effort is to demonstrate the potential role of acoustic cymbal transduction technology for Navy sonar applications by initially obtaining an understanding of depth dependent performance issues and then to investigate a hydrostatic pressure compensation system introduced for the first time. This research suggests that consistent and reliable acoustic performance can be achieved with cymbal-based transducers at hydrostatic pressures of interest to the Navy.

THIS PAGE INTENTIONALLY LEFT BLANK

## **I. UNDERWATER ELECTROACOUSTIC TRANSDUCERS**

Underwater electroacoustic transducers are devices with the specific purpose of converting acoustic energy in water into quantifiable electrical energy and/or vice versa. Design and engineering of such transducers for marine applications can be a complex science. The difficulties with designing a transducer to perform in an expected application are complicated by consistent and repeatable fabrication of the device (needed for array applications) and suitable acoustic calibration and electroacoustic evaluations in order to gauge understanding of the expected performance. The discipline required to fabricate a transducer type that performs in a consistent manner is inexact. Part of the reason is that transducer engineering and fabrication has not been formalized as a distinctive science in itself, but is instead an interdisciplinary blend of several and diverse sciences. Transducer design requires a working knowledge of acoustical physics, materials science, ocean/mechanical engineering, and electrical engineering. Some combination of applying these formal sciences is required to successfully obtain a transduction device and corresponding performance characterization that determines functional suitability for an underwater acoustics application.

### **A. SELECTED HISTORY**

For most modern underwater electroacoustic devices, capability resides with taking advantage of the piezoelectric effect. In Greek, the term piezoelectricity literally means “pressure electricity.” Although the naturally occurring piezoelectric effect in certain natural crystalline materials was discovered by Jacques and Pierre Curie circa 1880, the benefit from this phenomenon for underwater electroacoustic devices was not realized until much later. On 27 April 1914, two years after the catastrophic sinking of the *RMS Titanic*, a moving coil transducer, called the Fessenden oscillator as seen in Figure 1, successfully detected an iceberg nearly two and one half miles away by underwater echo-ranging [1]. Although the transduction mechanism of the Fessenden oscillator was not piezoelectric, it did magnify the value of underwater transduction concepts overall. And in 1917, a steel-quartz-steel resonator plate designed by French scientist Paul Langevin demonstrated a similar transduction response, but by utilizing the

piezoelectric effect instead. Langevin's efforts, however, were for a different purpose than detecting icebergs – the need to detect and locate German submarines was the primary motivation [2]. Even though the technology was developed too late in WWI to effectively detect the submarines, the motivation to be successful in this technology area remains to be an integral focus of Navy programs.

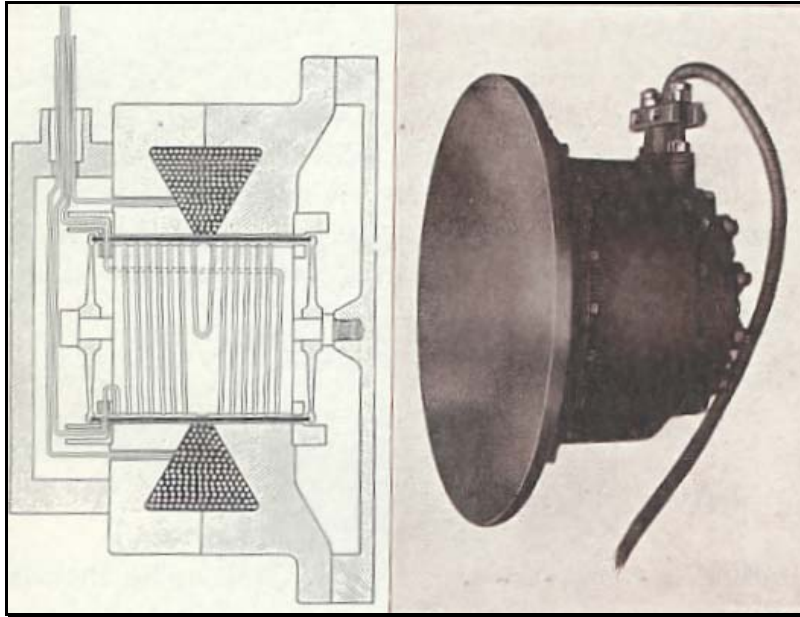


Figure 1. The “Fessenden Oscillator” from Ref [1]<sup>1</sup>

## **B. FLEXTENSIONAL TRANSDUCERS**

One distinctive type of electroacoustic transducer that has been featured in various Navy concepts and applications is the composite metal-ceramic flextensional type transducer. The configuration of such a transducer can be quite diverse and many of these designs undergo iterative changes to make them more efficient and reliable for an application. Flextensional transducers provide an advantage for acquiring considerable acoustic volume velocities, a requirement for low frequency operation, from relatively small devices. Classically, this has been achieved by means of larger, more expensive devices. Therefore, for some Navy applications, the flextensional transducer is still a transduction technology that remains an attractive option.

---

<sup>1</sup> Photograph taken from Raytheon Corporation's Submarine Signal Log

## 1. History of the Flextensional Transducer

The first flextensional transducer design was pioneered in the late 1920s by Harvey Hayes at the Naval Research Laboratory for use as a foghorn – an application for which it proved to be ill-suited [3, 4]. And an underwater flextensional transducer (called “Mod II”) obtained from Hudson Laboratories by Morton Kronengold and William Toulis, seen in Figure 2, was successfully used by in 1961 during experiments to study sound propagation near Miami, Florida.



Figure 2. Underwater flextensional transducer from Ref [4]<sup>2</sup>

Since the original design, seven primary classes of flextensional transducers have been developed, each class denoted by respective Roman numerals I through VII. The “cymbal transducer” is a miniature class V flextensional known also as a “ring-shell” design. Credit for the class V flextensional design, which was comprised of a ring of

---

<sup>2</sup> Groves, I.D., *Acoustic Transducers*

ceramic as the drive motor is attributed to Frank Abbot. A practical application for class V flextensional transducers was sonobuoys [5].

The concept of providing a compensation scheme for hydrostatic pressure experienced by flextensional transducers is not a novel idea. In 1955, Abbott submitted a patent involving flextensional transducers with concave and convex shells as well as for the injection of gas within the transducer in order to avoid the collapse of the flexural shells while at depth [5]. The principal factor for the lack of success was problematical fabrication.

## **2. Mechanics of Operation**

Though it is uncertain as to when the term “flextensional” was coined, it is derived from combining terminology that describe its composite function: a *flexural* vibration of the sound-radiating shell as mechanically driven by the positive *extensional* and negative *contractional* vibration components of the drive element [5], typically a piezoelectric ceramic element or stack of elements. The flextensional transducer consists of an electromechanical drive element bonded to a flexing shell. A class V flextensional transducer generally has two shallow convex (or concave) partly-spherical shaped shells with flattened flanges that are bonded to a thin piezoelectric disk or ring. Radial expansion and contraction in the disk or ring, by way of the piezoelectric effect, delivers strong radial forces on the attached curved shells. This radial force acts on the outer diameter of the shells to generate amplified axial motion perpendicular to the bond line [6, 7]. A flextensional transducer can produce large volume velocities and displacements to amplify efficiency and acoustic output at low frequencies for the size of the device [8]. As with other transduction technologies, this design concept can be scaled to large or small devices depending on the desired frequency of the application, as well as the desired force and velocity output of the device.

## **C. MINIATURE FLEXTENSIONAL CONCEPT**

The first miniature class V flextensional is the successful “moonie transducer,” known more commonly as the “*moonie*,” which was conceived during the 1980s at The Pennsylvania State University for hydrophone applications. The moonie is an inexpensive device made up of two metal endcaps that are bonded to a piezoceramic disk.



Each metal endcap has a shallow cavity machined into its inner surface similar to the shape of a crescent moon, hence its name. The moonie was later configured with polyethylene flexing caps and installed as the primary sensor in underwater towed line arrays used for geophysical research [9]. It is the most successful patent at The Pennsylvania State University to date [10]. However, when performance characteristics were investigated in detail, limitations became apparent.

Finite element analysis revealed large stress concentrations in the moonie endcaps near the bond layer that were causing reliability problems and restricted mechanical displacement. A new cap design was conceived to eliminate this stress concentration [11]. The resulting cap design geometrically resembles a percussion instrument, the cymbal, hence the current terminology – cymbal transducer – which is a miniature class V flextensional.

It is significant to note throughout this thesis that design objectives for each cymbal transducer component will eventually focus on maintaining a balance of a broadband frequency capability for military acoustic arrays even though the array analysis is beyond the scope of this study. Low volume, low frequency performance (to extend the bandwidth), passive and active modes of operation, and consistent performance with hydrostatic pressure (shallow, littoral, and deep-ocean) are the parameters that will be addressed. To understand this to sufficient detail, each of the components that make up the cymbal transducer will be examined.

THIS PAGE INTENTIONALLY LEFT BLANK

## II. ACOUSTIC CYMBAL ELEMENT COMPONENTS

The design and configuration for each of the components that make up the acoustic cymbal element is examined in the following sections.

### A. PIEZOELECTRIC DRIVER

As with every underwater electroacoustic transducer design, selecting the proper active driving element, commonly referred to as the *motor* or *actuator*, is fundamental to function and performance. The driving element typically incorporates a piezoelectric ceramic material.

#### 1. Piezoelectric Effect

Some materials are capable of producing an electric potential across two opposite surfaces as a result of mechanical stress. The *piezoelectric effect* is the phenomenon whereby this electric potential is proportionally generated within certain anisotropic crystalline materials when exposed to mechanical stress (like acoustic pressure). Conversely, mechanical deformation in these materials is generated in proportion to a limited electric field. Piezoelectricity is the measurable electrical potential resulting from the physical deformation that occurs within piezoelectric materials [12].

Discovery of this phenomenon has resulted in the implementation of naturally occurring piezoelectric crystals, together with synthetic ferroelectrics, as the active material in underwater transducers for receiving and projecting sound – with varying efficacy. By far the most commonly used piezoelectric materials are the piezoelectric ceramics, otherwise known as *piezoceramics*, a family of polycrystalline ferroelectrics. Polycrystalline ferroelectrics are identified as piezoceramics when they are in a polarized condition. Dissimilar to natural piezoelectric crystals, which have inherent piezoelectric behavior; piezoceramics offer the advantage of being shaped during the beginning stages of the manufacturing process into configurations for a particular application. The first of these materials, Barium Titanate ( $\text{BaTiO}_3$ ), was purportedly discovered independently by researchers in the United States, the Soviet Union, and Japan sometime in 1943 [12, 13]. It remained the leading piezoceramic material until the 1953 discovery of Lead Zirconate

Titanate ( $\text{Pb}(\text{Zr},\text{Ti})\text{O}_3$ ), which is still recognized by its original trade name *PZT*. PZT has since been the material of choice for most electroacoustic devices because the piezoelectric coefficients are nearly twice that of Barium Titanate [13].

## 2. Piezoelectric Relations and Crystallographic Structure

Piezoelectricity intrinsically provides a coupling between elastic and dielectric phenomena, which may be expressed in mathematical terms for elastic and electrical properties of the active material [12, 14]. Setting  $D$  as the *charge per unit area* (also known as dielectric displacement),  $T$  as the *mechanical stress*,  $E$  as the *electrical field*, and  $S$  as the *material strain*, the fundamental piezoelectric equations of state are given by the following equations,

$$\begin{aligned} D_m &= d_{mj} T_j + \varepsilon_{mn}^T E_n \\ S_i &= s_{ij}^E T_j + d_{ni}^t E_n \end{aligned} \tag{1}$$

where  $m, n = 1$  to 3 and  $i, j = 1$  to 6, the tensors are indicative of direction.

Material properties in these equations are the elastic modulus  $s_{ij}^E$  and the dielectric constant  $\varepsilon_{mn}^T$ . The piezoelectric charge constant is symbolized as  $d_{mj}$ . The dielectric constant term,  $\varepsilon_{mn}^T$ , is a second rank tensor, the piezoelectric constant term,  $d_{mj}$ , is a third rank tensor, and the elastic compliance term,  $s_{ij}^E$ , is a fourth rank tensor. Superscript  $E$  designates that an electrical short circuit condition (setting  $E = 0$ ) is used to determine the elastic modulus. Superscript  $T$  specifies that the dielectric constant ( $\varepsilon$ ) is measured under constant stress (setting  $T = 0$ ) which is known as the free condition and the clamped condition (setting  $S = 0$ ) indicates constant strain. An open circuit condition (setting  $D = 0$ ) is used to determine constant dielectric displacement [12, 15, 16, 17, 18]. PZT has a Perovskite crystal structure. The Perovskite name originally comes from the mineral  $\text{CaTiO}_3$  which displays this structure, but PZT is a structurally variant version. In the Perovskite unit cell for PZT, lead ions occupy the corners (A sites), oxygen the faces (X sites), and titanium/zirconium the octahedral voids (B sites). The titanium and zirconium ions are smaller than the octahedral void and therefore can be displaced by applying an electric field or mechanical load. The oxygen ions will simultaneously be displaced in the opposite direction of the titanium/zirconium ions [12, 19].

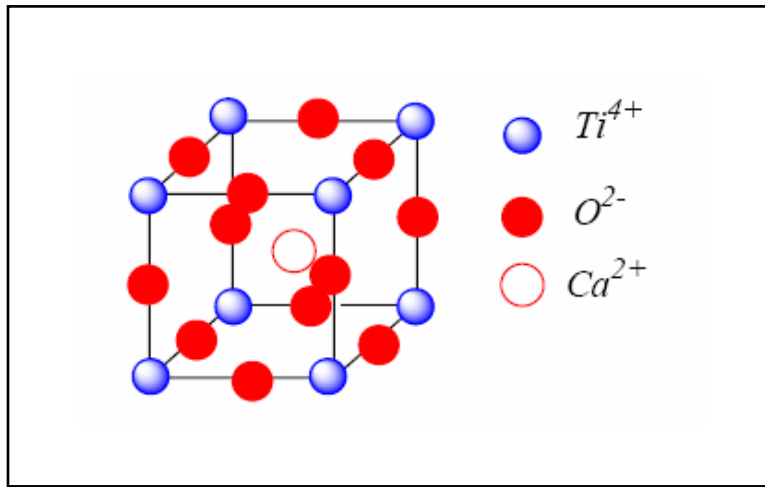


Figure 3. Representation of Perovskite structure for  $\text{CaTiO}_3$  from Ref [19]<sup>3</sup>

From an engineering science point of view, two types of piezoelectric constants are commonly used to express the relationship between electrical and mechanical parameters [20]. As discussed above, the electrical parameters of interest are charge density and electric field whereas mechanical parameters of interest are stress and strain. The piezoelectric voltage constant, symbolized by  $g_{ij}$ , is defined as a ratio of either *(mechanical strain)/(applied electric charge density)* – or – *(charge density)/(applied stress)*. The piezoelectric charge constant, symbolized by  $d_{ij}$ , is either the ratio *(strain)/(applied electric field)* – or – *(charge density)/(applied stress)*. For both of these constants, the subscript  $i$  specifies the direction normal to the electrode surface and the subscript  $j$  specifies the direction of induced strain or applied stress [20].

<sup>3</sup> <http://www.science.uwaterloo.ca.pdf>, February 2004

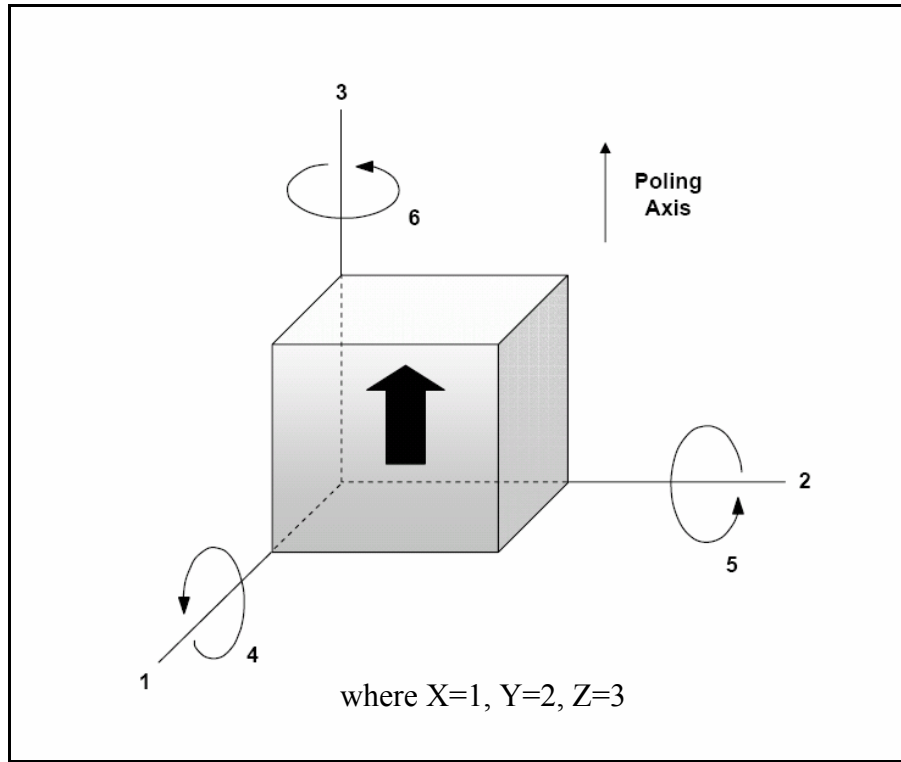


Figure 4. Illustration of piezoelectric parameter subscripts from Ref [20]<sup>4</sup>

These subscripts have integer values from 1 to 6. Subscripts 1, 2, & 3 define the three perpendicular directions; X, Y, & Z axes respectively as represented in Figure 4. Subscripts 4, 5, & 6 pertain to shear motion about these perpendicular directions. Additionally, the subscript *h* (for hydrostatic), is typically used as a subscript by itself (i.e.,  $g_h$ ) and is associated with simultaneous and equal stresses on all three axes similar to what is experienced by static pressures at various depths. These piezoelectric parameters are interrelated by the mathematical expression

$$d_{ij} = \varepsilon \varepsilon_o g_{ij} \quad (2)$$

where  $\varepsilon_o$  is the *permittivity of free space* ( $8.85 \times 10^{-12}$  Farads/meter) and  $\varepsilon$  is the *dielectric constant* of the piezoceramic and is established as the value in the poled direction, not as a variable vector quantity. The previously-mentioned definition of the

<sup>4</sup> [http://web.umn.edu/~rwschwar/Schwartz\\_Publications/Buchanan%20Figures.pdf](http://web.umn.edu/~rwschwar/Schwartz_Publications/Buchanan%20Figures.pdf), February 2004

piezoelectric voltage constant  $g$  emphasizes its role as a critical parameter for hydrophone sensitivity. Correspondingly, the piezoelectric charge constant  $d$  is a critical parameter for transmitting response [21].

### **3. Manufacturing of Piezoceramics**

Though the traditional science of manufacturing these materials is a mature one, maintaining uniform composition within any class of piezoceramics from one batch to another is still problematic. Additional to this, the possibility of nominal property value variations between manufacturers exists. Though some properties can be more tightly controlled typical military specifications may vary by as much as  $\pm 20\%$ , but at a higher cost. The piezoelectric constants, critical to the transducer designer, are a function of aging, temperature, humidity, frequency, and electric fields. Therefore, actual characterization is difficult because of the varied nonlinear properties [17]. For this reason, properties are reported with conditions.

The process of manufacturing piezoceramics starts with mixing appropriate quantities and ingredients of raw materials (Pb and oxidized Zirconate) and ball milling these raw materials. Next, the mixture is heated to 75% of the sintering temperature to accelerate reactivity within the mixture. The polycrystalline material is ball milled again to increase reactivity. The product is granulated together with a binder in order to improve the processing properties, formability and homogeneity, of the material. After shaping and pressing the shaped 'green' ceramic, it is heated to burn out the binder [17]. Controlling the tolerances of the parts during this phase is difficult for many piezoceramic providers.

The next phase of the process is sintering at high temperatures (usually between  $1250^\circ$  and  $1350^\circ$  C). The hard material is then cut, ground, and lapped to obtain the desired shape and tolerance wherever possible. Electrically conductive electrodes are applied by electroplating, sputter coating, or screen printing a conductive material (typically Ag) onto the surface. The initially manufactured ceramic material results in randomly oriented polarized regions. In this state, the material is classified as isotropic. The randomness precludes a usable piezoelectric effect [18].

To produce an anisotropic material from its initially manufactured state, the randomly oriented polarization directions are aligned by applying a voltage (>2000 V dc/mm) slightly below the Curie temperature for a brief period of time while immersed in a bath of non-conductive oil. Above the Curie temperature, the crystal structure converts to a centro-symmetric state and ferroelectricity is lost. The Curie temperature is the transition temperature from the ferroelectric phase to the paraelectric (non-ferroelectric) phase [22]. The resulting piezoceramic product is then cooled to room temperature. The cooled piezoceramic now has piezoelectric characteristics that are more or less permanently inherent. These characteristics are due to a net remnant polarization of the electric dipoles within the material structure [23]. And though imperfect, these dipoles are roughly aligned with the direction of poling. Groups of dipoles with parallel orientation are called Weiss domains [18]. Weiss domains may be degraded to an isotropic condition by exceeding the mechanical, thermal, or electrical limits of the material.

#### 4. Property Specifications

General properties of Navy piezoceramics are listed in Table 1 below [24, 25].

Table 1. General Properties of Navy Piezoceramic Types

Navy Types <sup>5</sup>		<b>I</b> (PZT4)		<b>II</b> (PZT5A)		<b>III</b> (PZT8)		<b>IV</b> (BaTiO <sub>3</sub> )		<b>V</b> (PZT6)		<b>VI</b> (PZT5H) <sup>6</sup>	
Property Name	Symbol	Typical Values	Aging Rate <sup>7</sup>	Typical Values	Aging Rate	Typical Values	Aging Rate	Typical Values	Aging Rate	Typical Values	Aging Rate	Typical Values	Aging Rate
Free Relative Dielectric Constant	$K^T_{33}$ *	1275 ±12.5%	-4.5 ±2.0	1725 ±12.5%	-1.5 ±0.7	1025 ±12.5%	-4.0 ±1.5	1275 ±12.5%	-1.50 ±0.5	2500 ±12.5%	-2.0 ±1.0	3250 ±12.5%	-2.0 ±1.0
Dielectric Loss Factor	$\tan \delta$	≤0.006	-	≤0.020	-	≤0.004	-	≤0.010	-	≤0.025	-	≤0.025	-
Planar Coupling Factor	$k_p$	0.58 ±8.0%	-2.0 ±1.0	0.6 ±8.0%	-2.5 ±0.15	0.5 ±8.0%	-2.0 ±1.0	0.30 ±8.0%	-1.5 ±0.50	0.63 ±8.0%	-0.25 ±0.2	0.64 ±8.0%	-0.25 ±0.2

<sup>5</sup> PZT nomenclature commonly used was added by the author.

<sup>6</sup> Type VI was never accepted into the DoD specification, but PZT5H is still referred by some as Type VI.

<sup>7</sup> The aging rate is typical change in properties up to 100 days after poling expressed in %/time decade.



Navy Types <sup>5</sup>		<b>I</b> (PZT4)		<b>II</b> (PZT5A)		<b>III</b> (PZT8)		<b>IV</b> (BaTiO <sub>3</sub> )		<b>V</b> (PZT6)		<b>VI</b> (PZT5H) <sup>6</sup>	
Piezoelectric Coefficient (x10 <sup>-12</sup> m/V)	d <sub>33</sub>	290 ±15%	-	390 ±15%	-	215 ±15%	-	140 ±15%	-	495 ±15%	-	575 ±15%	-
Planar Frequency Constant (Hz-m)	N <sub>p</sub>	2200 ±8%	1.3 ±0.8%	1950 ±8%	0.2 ±0.1%	2300 ±8%	1.3 ±0.8%	3150 ±8%	0.4 ±0.2%	1950 ±8%	0.35 ±0.2%	1940 ±8%	0.35 ±0.2%
Density (x10 <sup>3</sup> kg/m <sup>3</sup> )	P	≥7.45	-	≥7.60	-	≥7.45	-	≥5.50	-	≥7.40	-	≥7.40	-
Mechanical Quality Factor	Q <sub>m</sub>	≥500	-	≥75	-	≥800	-	≥400	-	≥70	-	≥65	-
% Change in K <sup>T</sup> <sub>33</sub>		9.5 ±3.0	-	25 ±10.0	-	9.0 ±3.0	-	5.0 ±2.0	-	30 ±10.0	-	40 ±10.0	-
Approximate Curie Temperature (°C)		325	-	350	-	325	-	115	-	240	-	180	-

Additionally, some industry manufacturers (Channel Products, EDO Western, Morgan Matroc, and others) have tabulated specific properties of their particular piezoceramic products. The properties available from publications by piezoceramic manufacturers are an important resource of data for transducer engineers. Table 2 shows properties of various piezoceramic types as published by Vernitron Corporation in 1988 [26].

Table 2. Vernitron Listing of Typical PZT Properties

Material*	PZT-4	PZT-8	PZT-5H
Coupling Coefficients			
k <sub>p</sub>	0.580	0.510	0.650
K <sub>33</sub>	0.700	0.640	0.750
K <sub>31</sub>	-0.330	-0.300	-0.390
K <sub>15</sub>	0.710	0.550	0.680
Piezoelectric Charge Constants (x10 <sup>-12</sup> m/V)			
D <sub>33</sub>	285	225	593
D <sub>31</sub>	-122	-97	-274
D <sub>15</sub>	495	330	741
d <sub>h</sub>	41	31	45
Piezoelectric Voltage Constants (x10 <sup>-3</sup> Vm/N)			

$G_{33}$	24.9	25.4	19.7
$G_{31}$	-10.6	-10.9	-9.1
$G_{15}$	38	-28.9	26.8
$g_h$	3.7	3.6	1.5
Figure of Merit			
$d_h g_h$	152	112	68
$\epsilon_{33}^T/\epsilon_0$ (@ 1 kHz)	1300	1000	3400
$\eta_m$ (@ 1 kHz)	0.004	0.004	0.025
Mechanical Quality Factor			
$Q_m$ (@ 1 kHz)	500	1000	65
$P$ (kg/m <sup>3</sup> )	7600	7600	7500
Curie Temp. (°C)	325	300	195
Elastic Constants – Short Circuit (x10 <sup>-12</sup> m <sup>2</sup> /N)			
$s_{11}^E$	12.3	11.5	16.4
$s_{33}^E$	15.5	13.5	20.8
Elastic Constants – Open Circuit (x10 <sup>-12</sup> m <sup>2</sup> /N)			
$s_{11}^D$	10.9	10.1	14.1
$s_{33}^D$	7.9	8.5	9.0

## 5. Piezoceramic Material Types Considered

To date, PZT has been the material of choice for cymbal transducers.

Piezoceramic material Navy type VI (PZT 5H) has been specifically considered for this investigation because of the high values of  $d_{31}$ , which is the primary drive parameter for extensional and contractional force components within the cymbal transducer. In typical acoustic projector and receiver applications, Navy Type I (PZT4) is often used because of its balance of piezoelectric constants for both transmit and receive. But, as described in Table 2, Navy Type VI has a larger  $d_{31}$  therefore this material is considered to be the lead contender for this application. Significant cymbal transducer research has been done and is still being done with 12.7 mm (0.5 inch) diameter x 1 mm (0.040 inch) thick discs and rings. Since individual components were available for this study, it was cost-effective to use the same size cymbal transducer elements in order to exploit the current knowledge base and expand performance data.

## **B. FLEXURAL SHELL**

### **1. Material**

Different shell materials have been investigated with varying levels of success. A titanium alloy has been shown to produce desired performance characteristics for the cymbal shell in underwater acoustic transducer applications. It was chosen for its performance balance of acceptable acoustic velocity and force. The primary attributes of this alloy are [27, 28]:

1. elevated strength-to-density ratio (high structural efficiency),
2. low density (roughly half the weight of SST, Ni, and Cu alloys),
3. exceptional corrosion resistance (superior resistance to seawater), and
4. excellent retention of properties at elevated temperature (up to 600°C)

Titanium (Ti) is the fourth most abundant metal in the world but has been perceived to be a difficult material to use for a variety of applications. This perception is propagated by failures to properly machine titanium and its reputation for being a material that is problematical to weld. Titanium alloys in general are poor thermal conductors. Heat generated during cutting does not quickly dissipate through the part as it does for many other materials, but instead tends to concentrate in the cutting area thereby tempering and dulling cutting tool edges. As the tool dulls, even more heat is generated, further shortening tool life and compromising close tolerances. Cymbal shells are fabricated by punching out titanium sheets to avoid this problem.

A general understanding of performance can be determined from the calculated resonance frequency of a flexural shell. Resonance frequencies for different types of materials and shell configurations were calculated to determine which material and configuration would provide optimal performance for a specific application and is shown in Figure 5 [7].

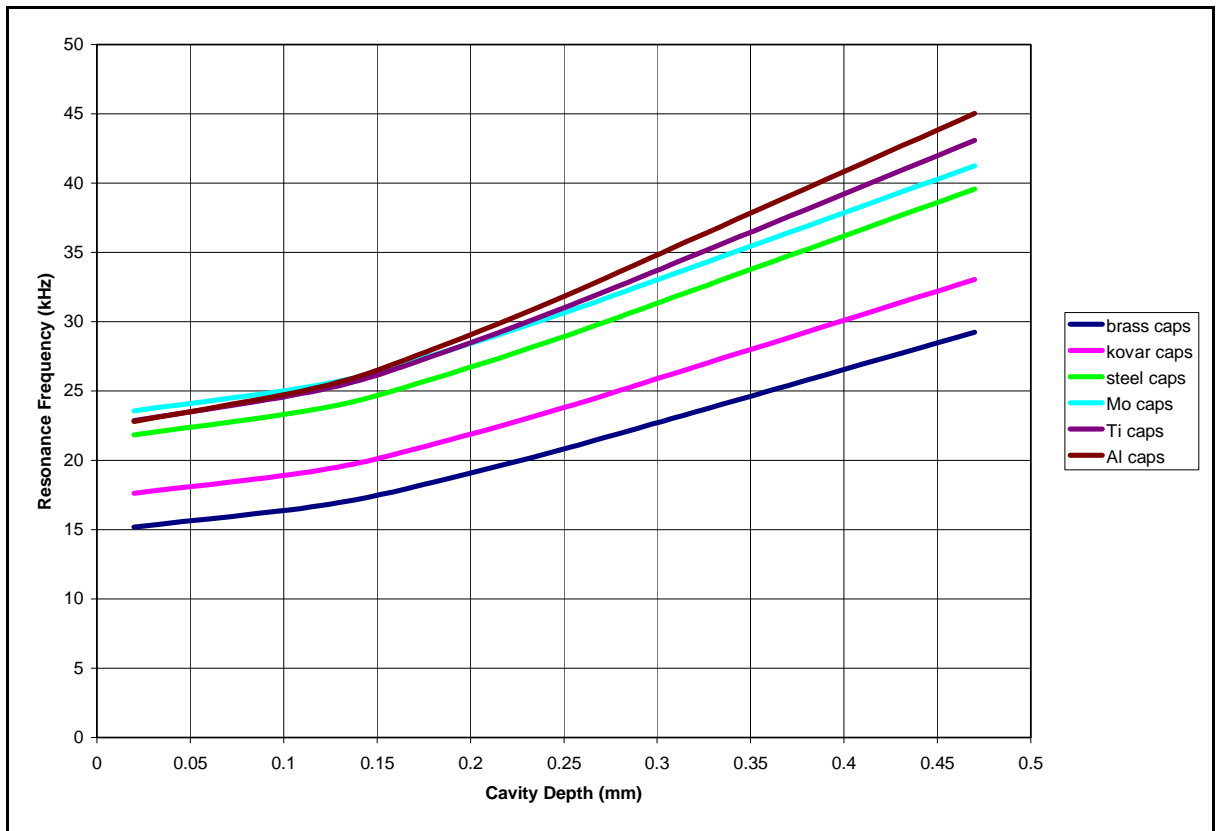


Figure 5. Resonance frequency (in-air) vs. cavity depth for various materials <sup>8</sup>

The cymbal shell for this study is made from a titanium alloy. This alloy was chosen for its strength to resist hydrostatic pressure, its light weight, and most importantly, its force and velocity profile as measured in situ.

## 2. Flexural Shell Configuration

Cavity and apex diameter as related to the cavity depth and diameter primarily affects resonance frequency. The influence of the cavity diameter and depth of the cymbal affects resonance frequency as shown in Figure 6 below. It is shown that cavity diameters provide a reasonable low frequency response at approximately 8 mm. This dimension relates to the depth of the cavity that was kept at a minimum, but large enough so there is no physical contact at the surface of the piezoceramic.

<sup>8</sup> As provided by Dr. J.F. Tressler at the Naval Research Laboratory in Washington D.C.

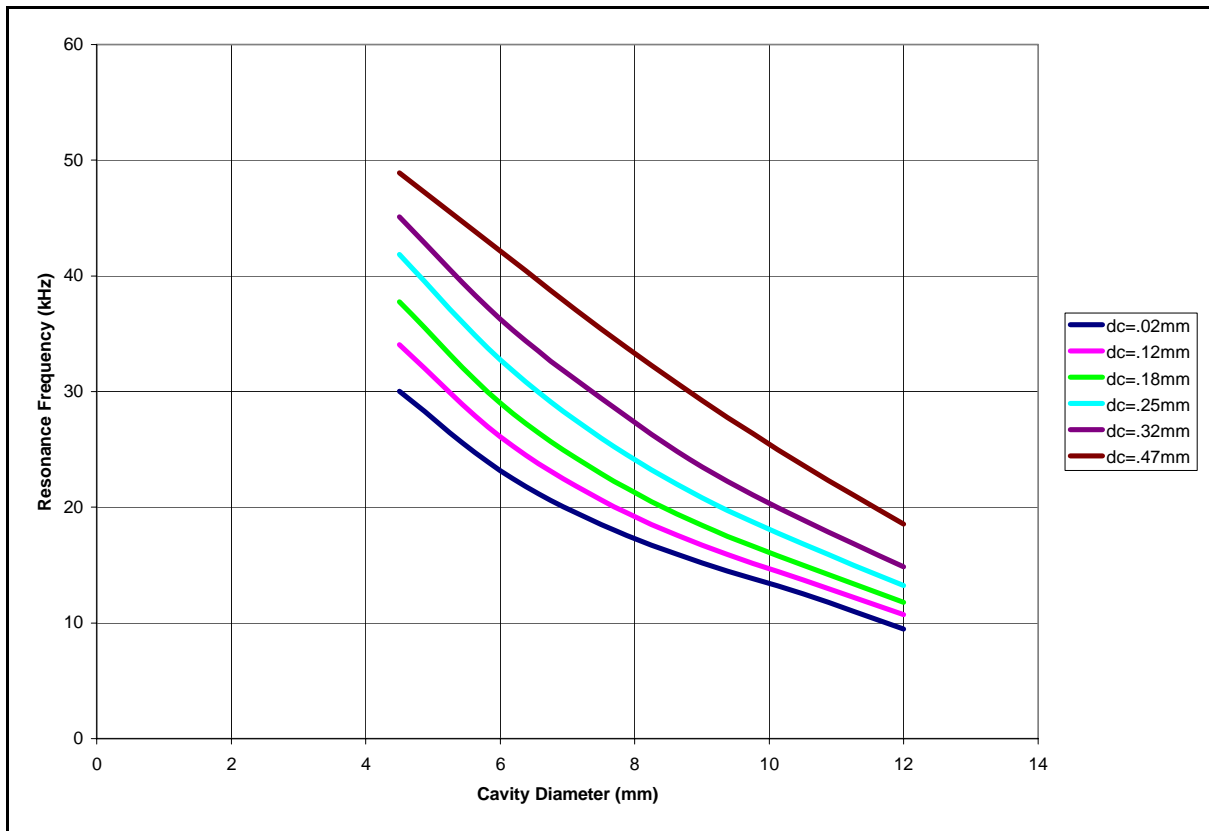


Figure 6. Resonance frequency (in-air) vs. cavity diameter - related to cavity depth<sup>9</sup>

The depth was chosen to be 0.6 mm (0.025 inch) to achieve a balance of maximum mechanical deformation (maximum displacement and velocity) and a low profile. Alternatively, the apex diameter is significant to the resonance frequency. Figure 7 shows some calculated values of the resonance frequency as it relates to the apex diameter and the cavity depth [13].

<sup>9</sup> As provided by Dr. J.F. Tressler at the Naval Research Laboratory in Washington D.C.

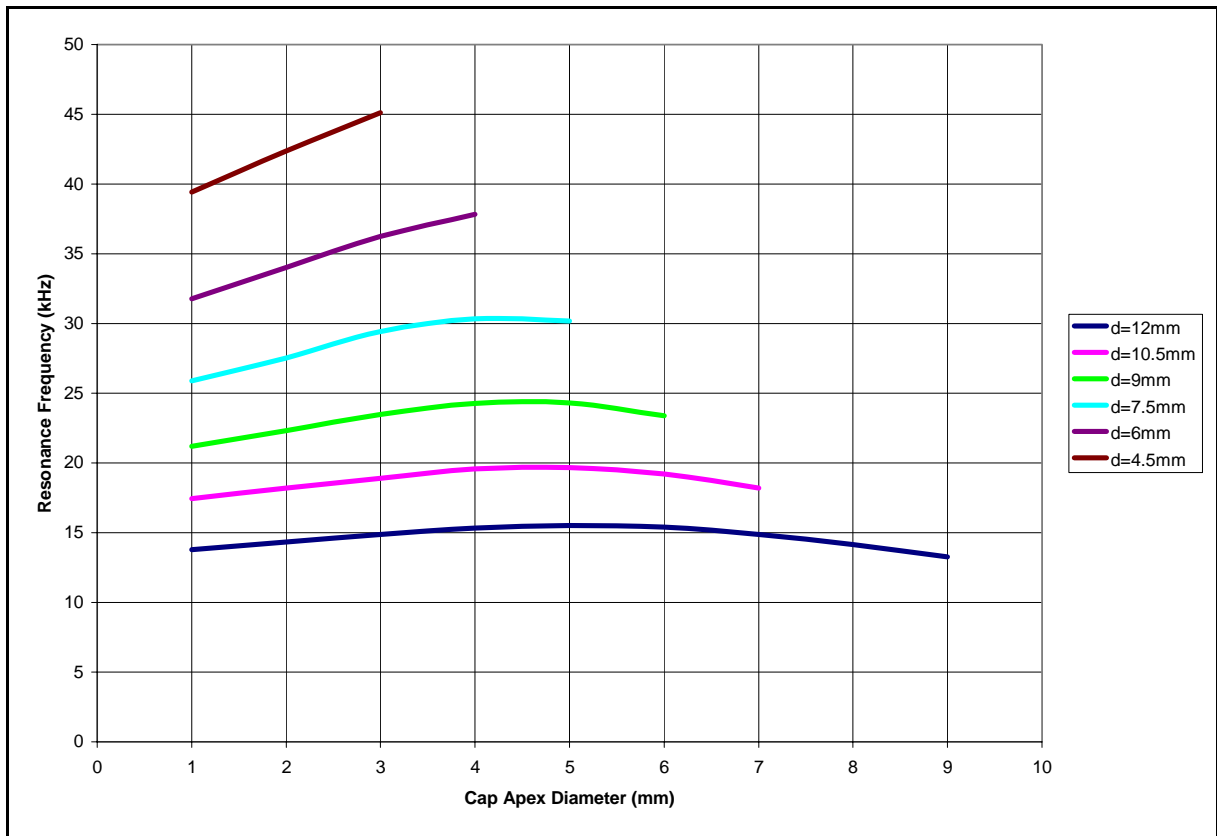


Figure 7. Resonance frequency (in-air) vs. apex diameter - related to cavity diameter<sup>10</sup>

### 3. Manufacturing

To fabricate an individual cymbal shell, a flat round sheet of the titanium is laid out and centered on a stamping die. Once the die has been tooled, components are easily reproduced and relatively inexpensive. The stamping die creates consistently-shaped flexural caps with a consistent configuration. But the stamping process produces a work-hardening effect in the titanium. Work hardening results in a resistance to plastic flow. When work is performed on a metallic piece below hot working temperatures, the crystal structure is forced to deform to accommodate the strain, microscopic shearing (or slip) occurs along definite crystalline planes. Discontinuities in the crystal structure, known as dislocations, increase in density during plastic flow and those moving on intersecting slip planes tangle and pile up. Eventually the stress required to move dislocations is high enough for a crack to initiate and subsequently propagate, the material starts to stretch and then finally fails [27, 28].

<sup>10</sup> As provided by Dr. J.F. Tressler at the Naval Research Laboratory in Washington D.C.

### C. EPOXY AND BOND JOINT

The problem of obtaining an optimal epoxy used for the bond joint that exists between the cymbal shells to the piezoceramic continues to be studied. The consistent mechanical and corresponding electrical functionality of this bond is significant to obtaining uniform performance from one cymbal to the next. The epoxy must have significant shear strength, some mechanical damping properties, and adequate electrical conductivity. And though uniformity is not critical to the results of this specific research, it is critical to array applications. Thicknesses of the bond joint vary with epoxy type, but the widths of the bond can be approximated by previously published data. The following data helped to determine some optimal bond widths [13].

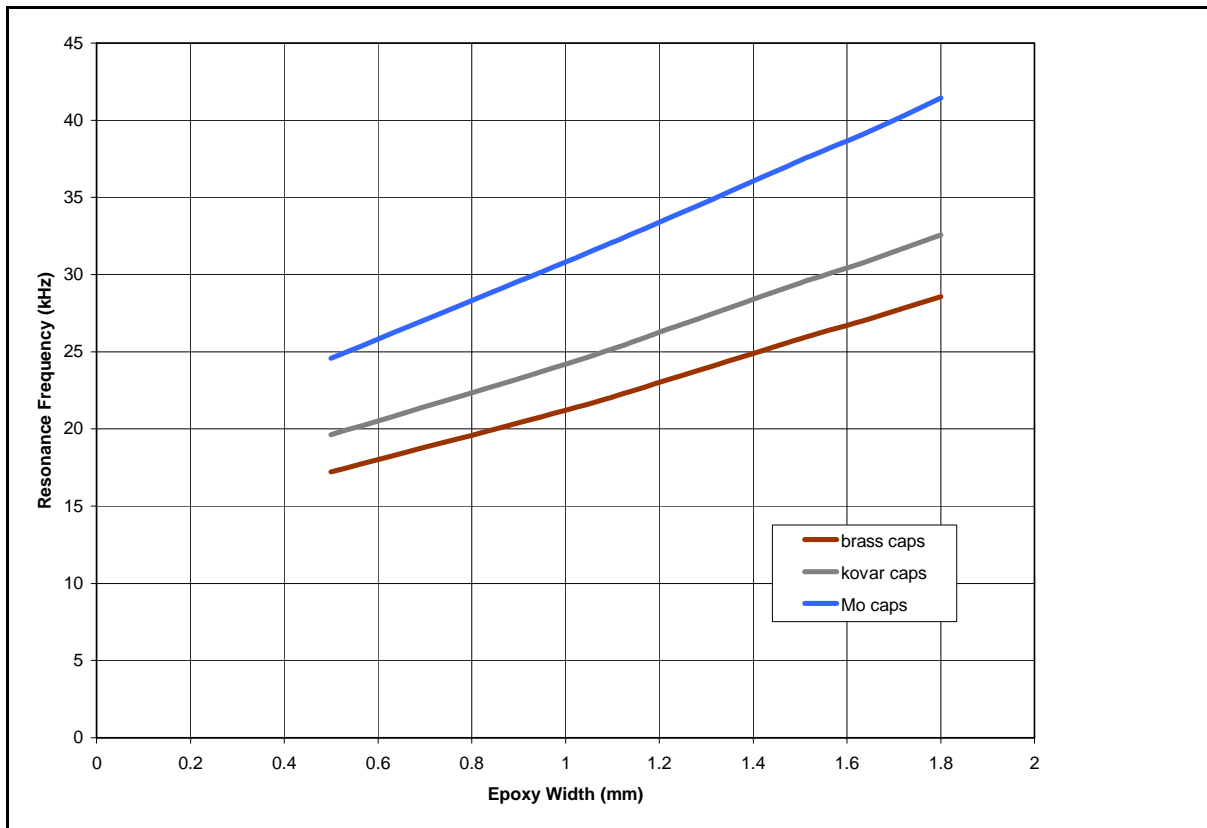


Figure 8. Resonance frequency (in-air) vs. bond line width<sup>11</sup>

Based on these results, the bond line thickness was chosen to be 1.8 mm (0.070") to maintain a high resonance frequency, thereby preserving broadband capability. The

<sup>11</sup> As provided by Dr. J.F. Tressler at the Naval Research Laboratory in Washington D.C.

strength of this bond was verified via a bond strength test on an Instron mechanical pull tester. The data from this test is shown in Figure 9 below.

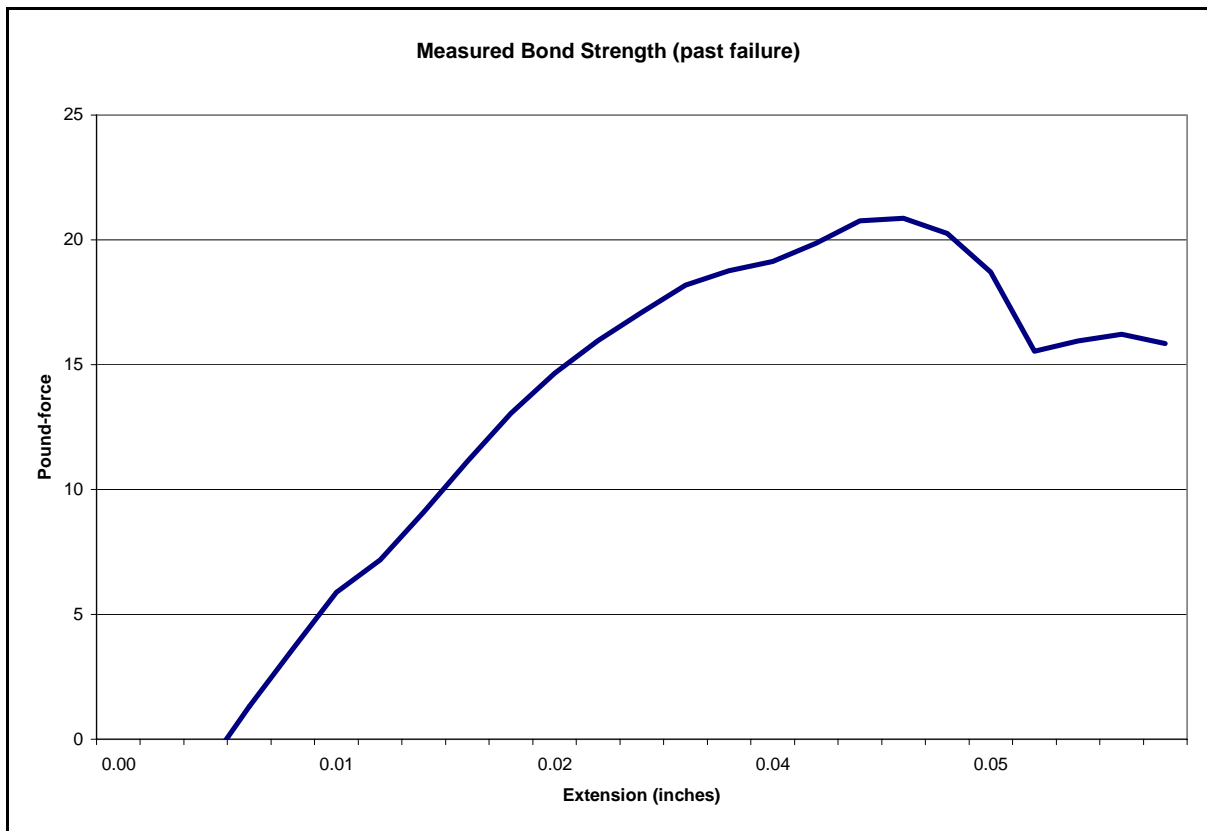


Figure 9. Instron pull test on cymbal shell to determine strength<sup>12</sup>

The strength of the particular cymbal element design tested was greater than 20 pounds of force which is orders of magnitude greater than any anticipated force in an application. In fact, the actual failure occurred at the apex of the flexural shell, not at the bond line between the shell and the piezoceramic. Thorough testing has revealed that obtaining a consistent and durable bond in such a delicate device is highly dependent on the care taken during the manufacturing and preparatory process with an application of a closely controlled amount of the proper bonding agent. Failure to closely regulate any facets of the aforementioned variables will affect underwater acoustic performance.

---

<sup>12</sup> Testing performed at NUWC laboratory in January of 2003



### III. FABRICATION OF ACOUSTIC CYMBAL ELEMENTS

Fabricating an acoustic cymbal element that performs in a predictable and consistent manner is the crucial evolution from design to the acoustical evaluation process. As stated earlier, consistent results are required especially for elements that will be installed in an array configuration. This section addresses the process of fabricating a commonly referenced Navy acoustic cymbal element.

#### A. FLEXURAL SHELLS

Initially, the cymbal shells are stamped into the prescribed configuration as shown below in Figure 10. The size of this particular cymbal shell is 0.5 inches (12.7 mm) in diameter x 0.010 inch thickness (0.254 mm) x 0.035 inches high (0.89 mm) with a 0.11 inch (2.79 mm) diameter apex (inside dimension).



Figure 10. Three views of titanium cymbal shells

#### B. TITANIUM STUD AND WELDMENT

For the Navy Standard cymbal element, the next step is to affix a threaded titanium mounting rod to the apex of both cymbal shells. The 0.20 inch long titanium threaded rod (size 0-80) is stud welded perpendicular to the flattened apex of the cymbal. The process of welding the stud in place on the cymbal shells is called *electron fusion*,

developed in 1963.<sup>13</sup> Electron fusion is a process that can quickly and effectively welds studs to a surface without damage to the substrate. Arc Stud Welding involves the same principles and metallurgical aspects as other arc welding procedures, in that a controlled electric arc is used to melt the end of the stud or electrode and a portion of the base metal. Because the parts are very small, very controlled conditions are important for this application. A small protrusion, called a nib is machined on the titanium stud. As the nib is pushed quickly down on the substrate of the titanium shell, it vaporizes from current caused by a high voltage capacitor, which causes a plasma arc between the stud and the shell. The stud is pressed quickly into the melted substrate (approximately 0.002 inches deep) and creates a strong and clean weld joint.

The threaded rods used for this process, shown in Figure 11, are purchased with a nib. This sharp point permits precise positioning of the electrical arcing required to produce the molten metal joint at the cymbal shell surface.



Figure 11. Two studs used for welding to center of apex

The base of the threaded rod that supports the stud, known as the fluxed end, is clearly seen on one end of each of the two rods. A special collet on the welding apparatus holds the stud firmly perpendicular to the substrate while a high voltage arc is emitted between the stud and the shell. This collet can be seen in Figures 12 (overall view) and 13 (close up view) on the base of the welding apparatus.

---

<sup>13</sup> Found on website for Contract Fusion at [www.contractfusion.com](http://www.contractfusion.com)



Figure 12. Stud welding apparatus

At the end of an automatically timed interval (approximately 0.2 seconds), the molten end is forced quickly against the molten metal pool on the shell. This series of consistent intervals provides a consistent and robust welded fillet [29].



Figure 13. Placing stud in the collet

After positioning the post in the collet, shown in Figure 13 above, the fluxed end of the threaded post is welded to the cymbal shell and allowed to cool to a solid state.

### C. ASSEMBLING THE CYMBAL SHELL

The resulting assembly is prepared for bonding to the ceramic disc by lapping the bond surface in a figure-8 pattern on superfine grit sandpaper as seen in Figure 14.



Figure 14. Lap bonding surface of flange to remove burrs

This portion of the assembly is washed in an alcohol solvent to remove dust and other residual contaminants. Multiple pieces can be fabricated to establish manufacturing efficiency. The flange of the subassembly is coated with a conductive epoxy prior to mounting it in an assembly fixture. It is critical that the amount of epoxy is carefully controlled. The cymbal shell is then placed into a fixture so the threaded post is positioned downward. A clean piezoceramic disk, with an epoxy ring on one side, is placed carefully on top of the cymbal shell as seen in Figure 15 below.

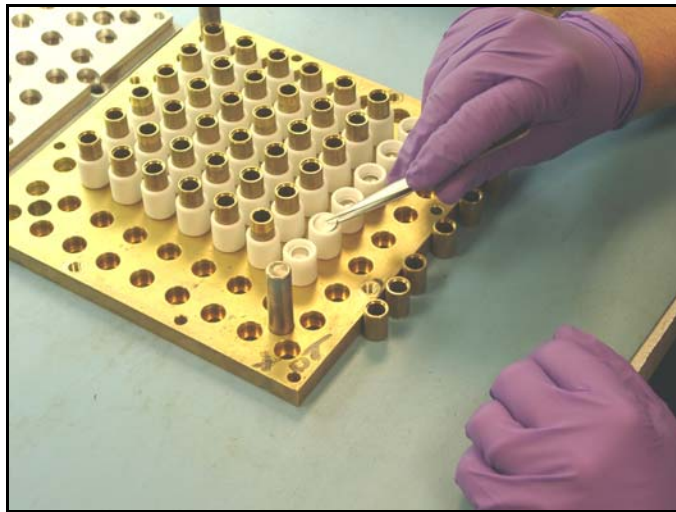


Figure 15. Epoxy coated piezoceramic is placed into assembly fixture

The process is then repeated for the other side of the piezoceramic to assemble the second cymbal shell. A metal plate is bolted in place to confine the final assembly for curing as

seen in Figure 16. Spring washers in each chamber of the assembly ensure a consistent compressive force on the assemblies.



Figure 16. Top plate being bolted into place

#### **D. FINAL STAGE OF ASSEMBLY**

The fixture with the cymbal assemblies is heated to shorten the curing process time to approximately one hour. After cooling, the cymbal elements are removed from the fixture and tested in-air in order to verify consistent quality. The cymbal elements are then removed prior to reaching equilibrium with the room to mitigate the risk of potential damage. Allowing them to reach room temperature prior to removal from the fixture can result in internal stress damage in the bond and/or the piezoceramic disk during the extraction procedure.

#### **E. MOUNTING FIXTURE FOR ACOUSTIC TESTS**

The mounting fixture, referred to also as the test platform, was created in order to secure the individual acoustic cymbal elements in place during acoustic characterization. Flexibility to test more than one acoustic cymbal element at a time is a desirable feature because acoustic validation and calibration is a time-consuming, and therefore costly, venture. The acoustic test platform, as shown in Figure 17 below, permits the time-saving flexibility to test more than one cymbal element configuration at a time.



Figure 17. Acoustic test platform for cymbal elements

The test platform consists of two rigid metal rods (positioned  $90^\circ$  from direction of calibration measurement) that are brazed into bronze metal endcaps. Between the two rods is a molded rubber mount that holds up to five individual cymbal elements at a time. The rubber mount holds the cymbal elements in place nodally so the extensional and contractional movements are not restricted (simply supported boundary condition). Not shown in Figures 18 and 19 is the rubber acoustic window (a ‘boot’ made from a specialized acoustically transparent molded neoprene) that encloses the rods, rubber mount, and cymbal elements.

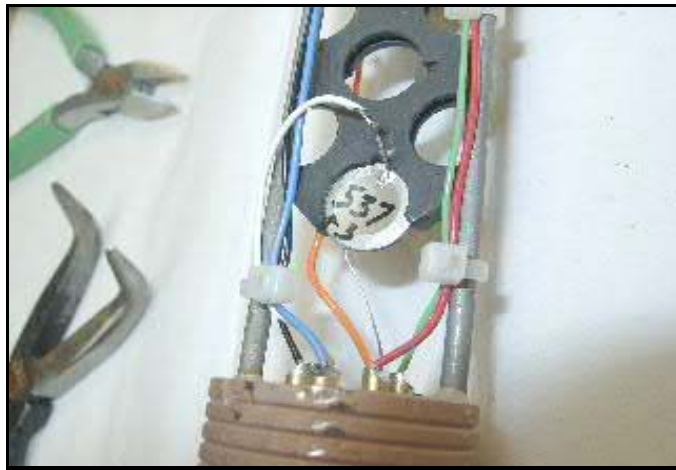


Figure 18. Close-up of cymbal element in acoustic test fixture

A threaded thru-hole allows for the test platform to be filled with evacuated castor oil which provides ample acoustic coupling between the acoustic cymbal elements and



the water. For electrical signal leads (driving and receiving), a high-pressure 6-pin bulkhead connector is threaded into a bronze endcap to electrically access the cymbal elements individually.



Figure 19. Author installing acoustic cymbal transducers

Five of the six pins are for the high side (+) of each cymbal element with the sixth pin (counting CW) used as a common ground (−). The bulkhead connector mates with a molded connector at the end of a 20 meter long cable. The cable leads at the dry end are marked individually as positions 1 through 5 in order to keep track of the relative locations of each cymbal element configuration.

THIS PAGE INTENTIONALLY LEFT BLANK



## IV. IN-AIR EVALUATION OF CYMBAL ELEMENTS

Characterizing transducer elements in-air prior to determining underwater performance may be conducted on some or all elements prior to implementation into an array. The purpose of doing so is to establish a baseline of performance and understanding for acoustic cymbal elements. Also it will help to ensure that element parts and assembly processes have, as the end result, produced a consistent product that matches from element to element. Discussions about typical in-air testing, such as impedance analysis and an atypical method, Scanning Laser Vibrometry (SLV), of acoustic cymbal elements follow.

### A. IMPEDANCE AND ADMITTANCE

For many years, generating “*impedance loops*” was the generally accepted method to gain understanding about a transducer element frequency response. Massaging the data in these impedance loops in order to obtain a representation of data in a relevant manner is time-consuming and inaccurate as compared to the capability of more recent digital equipment that is available in state-of-the-art transducer laboratories. Though some in the industry still prefer to use impedance loops, these impedance loops are being used in a lesser capacity to characterize transducers. Many transducer elements are currently being characterized more quickly by means of equipment such as the HP4194A Impedance/Gain-Phase Analyzer; an instrument designed for this purpose specifically [30]. The HP4194A provides a graphical display of impedance or admittance vs. frequency with or without electrical phase as well as many other features. It has been around for a couple of decades, is easy to use, and provides Impedance-Phase data very quickly and accurately.

Electrical impedance ( $Z$ ) is the ratio of voltage to current in an electrical circuit; a complex (two part) quantity. The real part is resistance ( $R$ ) and the imaginary part is the reactance ( $X$ ) of an electrical circuit and is related in the following manner [31]:

$$|Z| \equiv \sqrt{R^2 + X^2}. \quad (3)$$

Admittance ( $Y$ ) is defined as the reciprocal of impedance, hence,

$$Y = (Z)^{-1}. \quad (4)$$

Either admittance or impedance can be used to characterize an acoustic cymbal element.

### 1. Admittance Data

Admittance data can be acquired by way of the HP4194 for evaluation of a cymbal element. In Figure 20 below, admittance and admittance phase was collected from 10 kHz to 100 kHz. Resonances can clearly be seen at approximately 14 kHz, 16.5 kHz, 71 kHz, and 76 kHz. The 16.5 kHz resonance is not typical of a cymbal element. And even though the cymbal element may not be used in the upper frequency regions as measured, the data can still be used to verify and compare consistent performance of fabrication (materials and process) for each cymbal element.

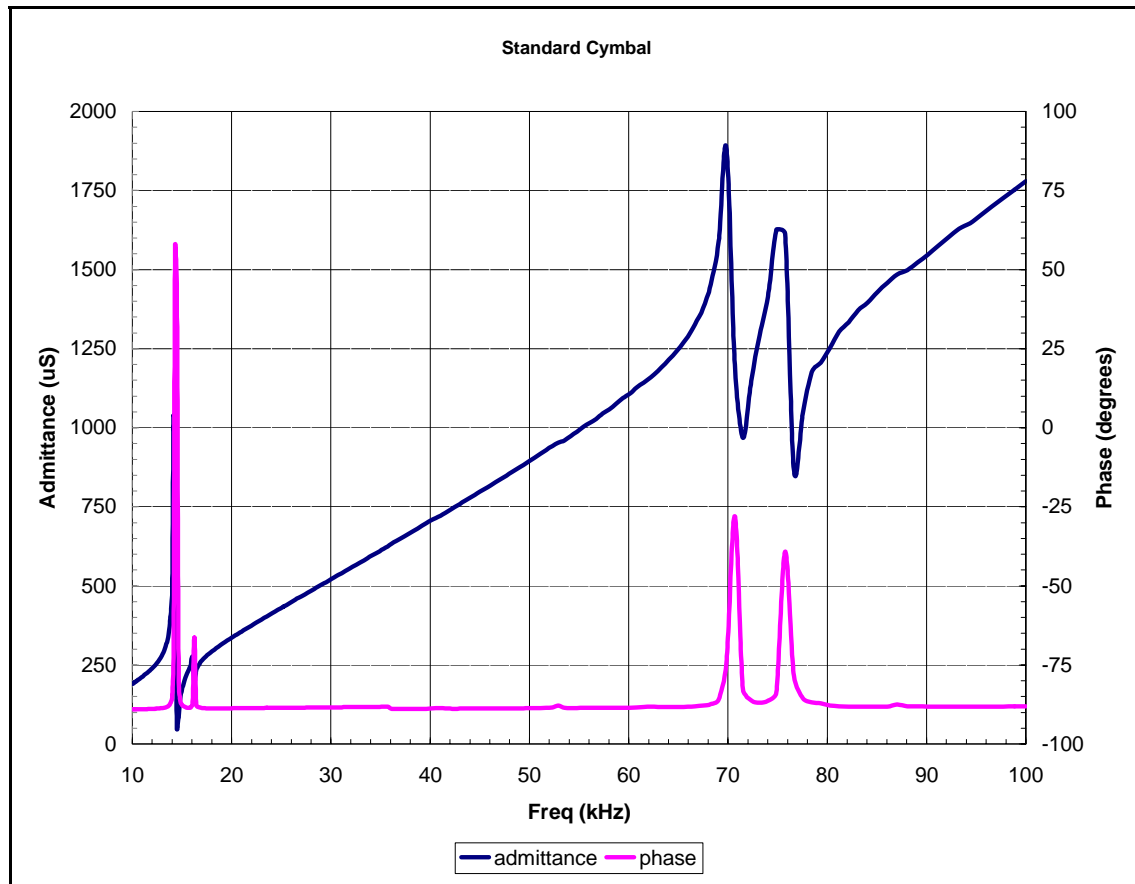


Figure 20. Admittance plot (with phase) of acoustic cymbal element

### B. SCANNING LASER VIBROMETRY

Scanning laser vibrometer (SLV) systems consist of an optical instrument (scanning laser), video display, and a computer to record data that provides an accurate, qualitative visual image of the spatial and temporal distribution across a vibrating structure. The optic head, mounted on a tripod, is adjusted relative to the user-defined vibrating structure. Vibration data from thousands of individual points (depending on the resolution available) is automatically recorded and merged in order to generate a graphical image that reflects the velocity and displacement of the vibrating surface. Some of the benefits of SLV are that the Doppler frequency shift of the laser wavelength allows for very high accuracy without disruption of the vibrating surface [32]. This non-disruptive process of measurement allows the user to observe actual behavior, predicted and unpredicted. This is the first time that vibration modes of individual cymbal elements have been observed by way of SLV. Though more than 800 computer files were generated, only a few representations are provided to help show some of the many flexural modes.

## **1. Test Equipment and Interpretation of Data**

While driven with a relatively mid-range voltage ( $\sim 50 V_{\text{rms}}$ ), the acoustic cymbal element flexural surface was scanned with a SLV at the Naval Undersea Warfare Center's (NUWC) Acoustic Test Facility (ATF). The purpose was to gain insight into the structural vibrations in a driving condition. The acoustic cymbal element was mounted from a common laboratory fixture with very light wires attached to each of the threaded titanium rods (free-free boundary condition). The wires provided a means to mechanically hang the acoustic cymbal in place and also provided the means to drive the acoustic cymbal element with a voltage of  $50 V_{\text{rms}}$  at different frequencies. Both velocity and displacement were recorded within the central frequencies of interest (2 kHz (low end), 14 kHz (in-air resonance), and 30 kHz (high end)). A measurement was also performed at 40 kHz because of noted behavioral changes.

Except for the data taken at 40 kHz, all test results in the following sections are displayed in three dimensional representations of the displacement that the cymbal element experiences while being driven at  $50 V_{\text{rms}}$ . Though not very accurate, displacement and velocity ranges taken from the color coded data are provided. SLV is

not ideal for determining performance of acoustic cymbal elements in water, but does provide a general understanding of the flexural modes in-air that may be transferred to performance underwater.

## **2. SLV Measurement at 2 kHz**

The measurement of the cymbal element in-air at 2 kHz shows that the movement of the flexural shell is very similar to a fundamental mode. The flexing shell moves more or less uniformly in and out from the position of equilibrium. This type of flexing movement is expected at frequencies at or below the fundamental resonance. The maximum range of displacement in the flexing shell is equal to  $\pm 0.35$  mm from equilibrium. The maximum range of velocity in the flexing shell, where maximum velocity occurs at the equilibrium position, is equal to  $\pm 5$  mm/sec. Figures 21 and 22 show the computer generated representation of displacement in the contractional and extensional modes respectively.

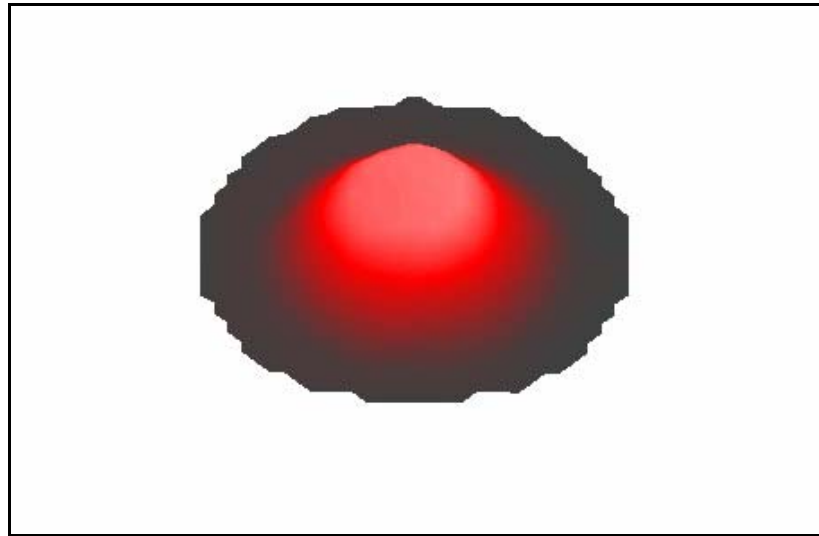


Figure 21. 2 kHz laser scan of cymbal shell in 3-d, contractional mode

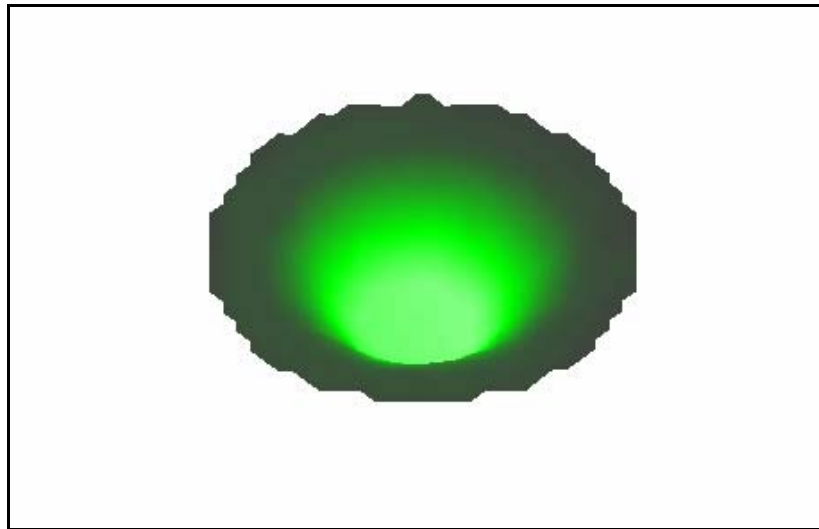


Figure 22. 2 kHz laser scan of cymbal shell in 3-d, extensional mode

### 3. SLV Measurements at 14 kHz

The measurement of the cymbal element at 14 kHz, the in-air resonance, shows that the movement of the flexural shell is, like at 2 kHz, very similar to a fundamental mode. The flexing shell center moves comparatively uniformly in and out from the position of equilibrium. Close examination of the image, and comparison with the 2 kHz image, shows that the apex of the flexural shell has a more exaggerated and defined displacement from equilibrium. The maximum range of displacement in the flexing shell is equal to  $\pm 0.5$  mm from equilibrium. The maximum range of velocity in the flexing shell velocity is equal to  $\pm 40$  mm/sec. Figures 23 and 24 show the computer generated representation of displacement in the contractional and extensional modes respectively.

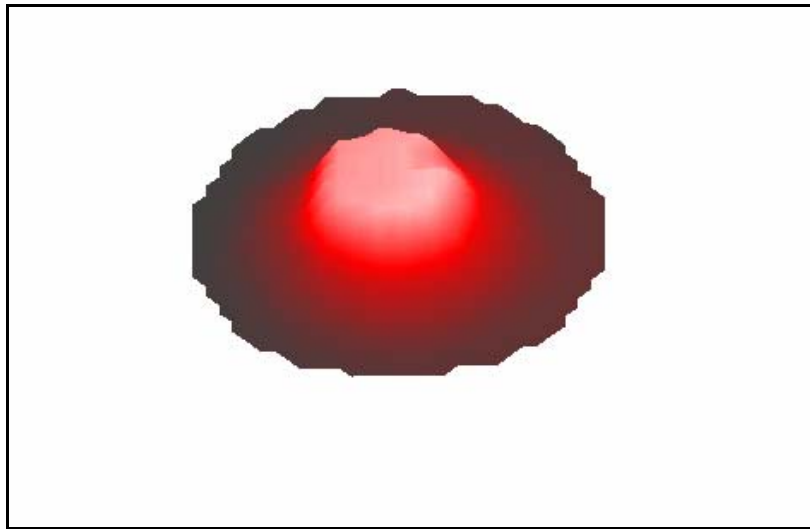


Figure 23. 14 kHz laser scan of cymbal shell in 3-d, contractional mode

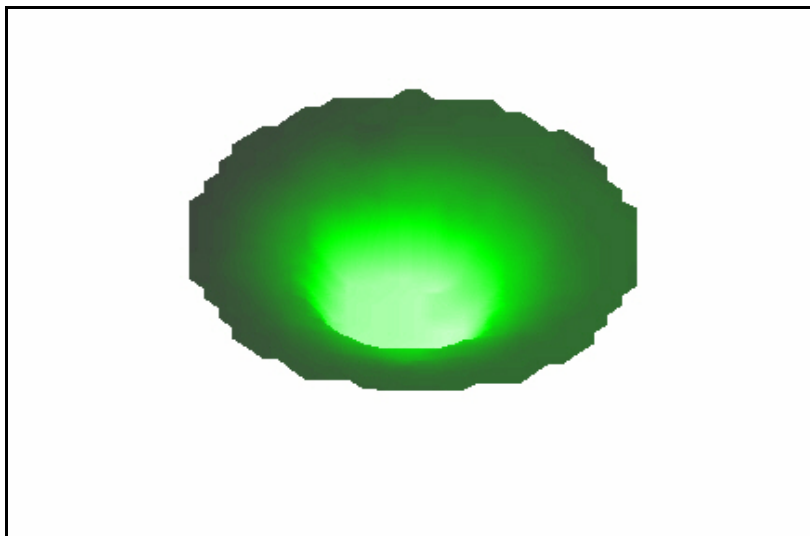


Figure 24. 14 kHz laser scan of cymbal shell in 3-d, extensional mode

#### 4. SLV Measurement at 30 kHz

The measurement of the cymbal element at 30 kHz, the high frequency for most of the in-water measurements, shows that the movement of the flexural shell is, unlike 2 kHz and 14 kHz, shifted to a different flexural mode. The flexing shell center moves 180° out of phase with the ring of surface area closest to the bond joint as seen in Figures 25 and 26. The maximum range of displacement in the flexing shell is equal to  $\pm 120 \times 10^{-3}$  mm from equilibrium. The maximum range of velocity in the flexing shell velocity

is equal to  $\pm 20$  mm/sec. Figures 25 and 26 show the computer generated representation of displacement in the contractional and extensional modes respectively.

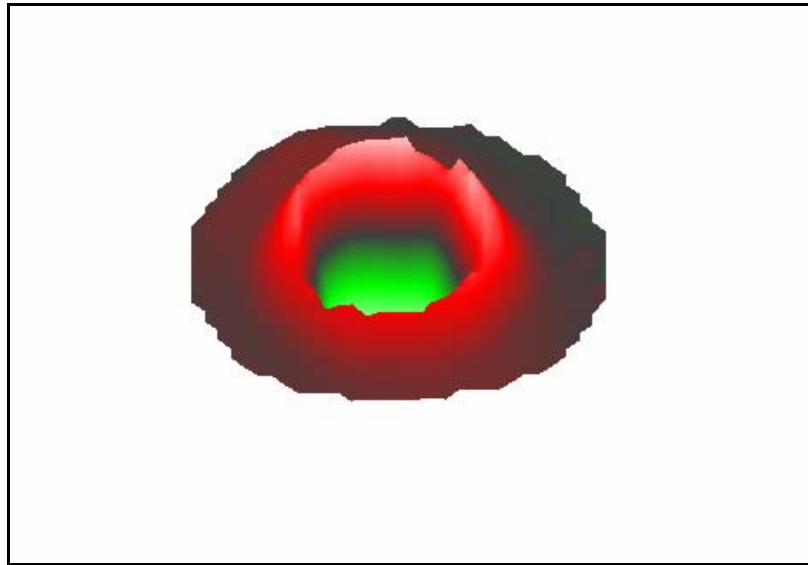


Figure 25. 30 kHz laser scan of cymbal shell in 3-d, contractional mode

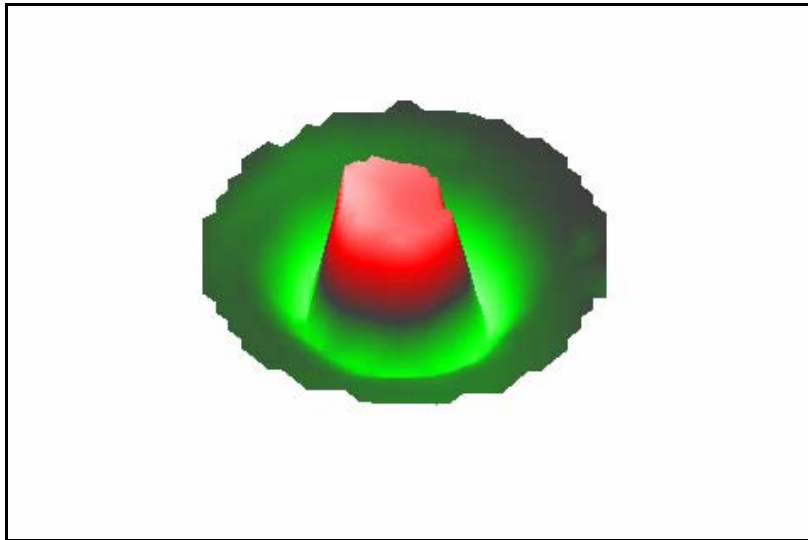


Figure 26. 30 kHz laser scan of cymbal shell in 3-d, extensional mode

## 5. SLV Measurement at 40 kHz

At least two modes of vibration were found to occur simultaneously at 40 kHz. One of the modes found at 40 kHz is similar to the flexural mode observed at 30 kHz. Another flexural mode (seen by alternating displacements at the circumference in Figure 27) was found to move circumferentially around the flexing shell. A two dimensional

representation of the modes is shown in Figure 28. Although this was not in the frequency band of interest for the acoustic applications, this data does show the capability and quality of SLV for in-air evaluation of acoustic cymbals.

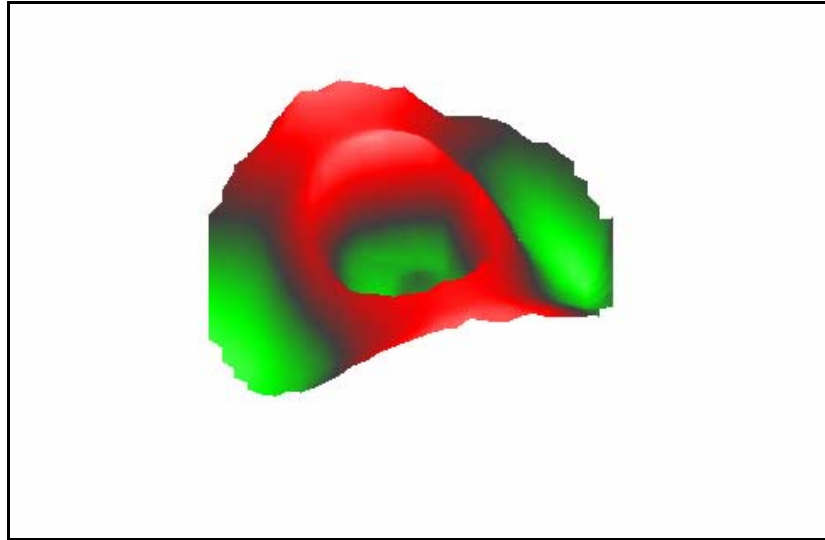


Figure 27. 40 kHz laser scan of cymbal shell in 3-d

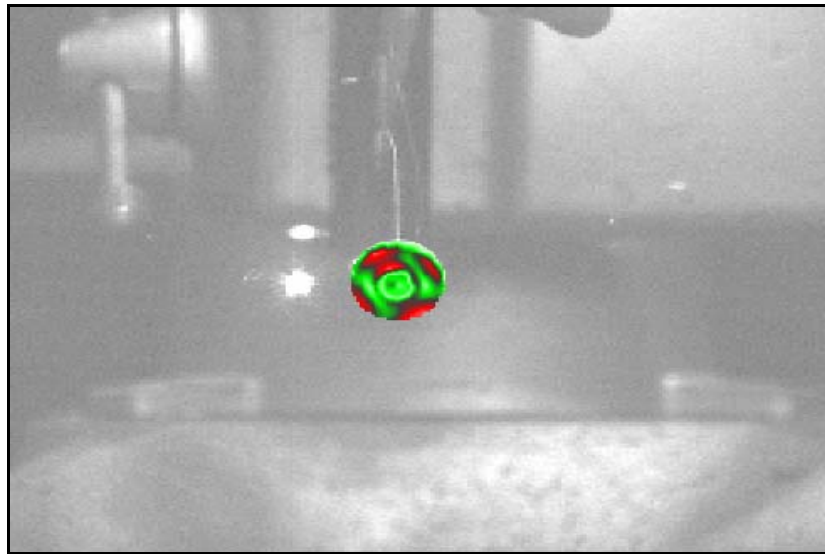


Figure 28. 40 kHz laser scan of cymbal shell in 2-d



## V. UNDERWATER ACOUSTIC MEASUREMENTS

Previous work on cymbal-based transducers has demonstrated reciprocal performance in applications as actuators and receivers [11]. However, acoustic cymbals are being used to function in a specific application in the U.S. Navy. That application is in an array being used for acoustic transmission [33]. Given both these positions, it is a point of completeness to measure the operation of each cymbal element configuration in both performance modes. Transmitting Voltage Response (TVR) for acoustic projectors and Free Field Voltage Sensitivity (FFVS) for receivers determine performance of a transducer by underwater acoustic calibration. Because accurate calibrations are high-priced, it is fortunate there is minimal effort involved to test each mode once the device and appropriate measurement hydrophones and/or acoustic sources are suitably rigged for measurements. Underwater acoustic measurements presented in this study are from a uniquely outfitted acoustic calibration facility that has the capability to characterize acoustic performance of transducers while they are concurrently exposed to hydrostatic pressure. Data logs and the transducer coordinates are available in appendices A–D.

The end result of electroacoustic measurements is the value obtained from a ratio of an electrical variable to an acoustical one and conversely, the acoustical variable to an electrical one [20, 21]. In underwater electroacoustic metrology, the typical ratios are sensitivity of a hydrophone reported in decibels (dB) relative to *Volts per Pressure* (dB reference 1 Volt per  $\mu\text{Pa}$  –or dB//1V/ $\mu\text{Pa}$ ) and the response of a voltage controlled acoustical projector reported in dB relative to *Pressure per Volt* (dB reference 1 $\mu\text{Pa}$  per Volt at 1 meter –or dB//1 $\mu\text{Pa}$ /V) extrapolated back to one meter away from the radiating surface. These parameters are characteristically represented by dB so accurate terminology for each is sensitivity *level* and transmitting response *level*.

### A. FREE FIELD VOLTAGE SENSITIVITY

Free Field Voltage Sensitivity (FFVS) of an electroacoustic transducer used as a receiver is the ratio of the output open-circuit voltage to the free-field sound pressure in

an undisturbed plane progressive wave. Sensitivity,  $M$ , of a transducer used in a passive mode is determined to be

$$M = \frac{e_{oc}}{p}, \quad (5)$$

where  $e_{oc}$  is the open circuit voltage and  $p$  is the free-field sound pressure typically expressed in terms of microPascal ( $\mu\text{Pa}$ ). A comparison calibration is used to determine the sensitivity of a hydrophone with an unknown sensitivity by comparing its output voltage,  $e_x$ , with an output voltage generated by a calibrated hydrophone standard,  $e_s$ . A hydrophone standard is characterized by stability and linearity within the measurement parameters [20]. The response of an ideal hydrophone standard would be independent of time, frequency, hydrostatic pressure, and temperature – otherwise the response must be defined within the boundaries of those same measurement parameters. Because the FFVS of the hydrophone standard is known, the unknown free-field voltage sensitivity,  $M_x$ , may be determined from the equation [20]:

$$M_x = \frac{M_s e_x}{e_s}. \quad (6)$$

Therefore, sensitivity of the unknown device can be expressed in decibels as:

$$20 \log M_x = 20 \log M_s + 20 \log e_x - 20 \log e_s. \quad (7)$$

## B. TRANSMITTING VOLTAGE RESPONSE

Transmitting Voltage Response (TVR) for an electroacoustic transducer is a calibration assessment of underwater acoustic projector performance in acoustic free field conditions referenced to a 1 V<sub>rms</sub> drive voltage. A definition of TVR for a transducer used to produce sound is the ratio of the sound pressure apparent at a distance of one meter in a specified direction from the effective acoustic center of the transducer to the signal voltage applied across the electrical input terminals [20].

By way of the reciprocity principle for underwater acoustic metrology (proved in 1946 by the Underwater Sound Reference Laboratory of Columbia University Division of War Research [20]), the transmitting response is proportional to sensitivity. Reciprocity states that the ratio of the receive sensitivity  $M$ , to the transmitting response  $S$ , must be equal to a constant  $J$ , called the reciprocity parameter [20].

The TVR of an acoustic projector presents an indication of performance when it is being assessed as a part of an acoustic system. The term *calibration* however, implies a free field condition which is difficult to achieve in a controlled environment such as a test tank. Therefore, transmitting response data is not necessarily a calibration, but is instead a measurement of the acoustic response to some electrical stimulus under specific environmental boundary conditions. To determine the transmitting response, a hydrophone standard with a known sensitivity  $M_s$  is placed some distance  $d$  away from the acoustic projector. The open circuit voltage from this standard is measured and recorded. The voltage response  $S_x$  can then be understood as [20]:

$$S_x = \frac{e_s d}{M_s e_x}. \quad (8)$$

And in deciBels this expression is

$$20 \log S_x = 20 \log e_s + 20 \log d - 20 \log M_s - 20 \log e_x. \quad (9)$$

### C. ACOUSTIC TEST FACILITY

To avoid the inherent difficulties and high costs associated with going to sea in order to understand low frequency acoustical behavior of a transducer while exposed to elevated hydrostatic pressure; acoustical calibration is typically performed in a laboratory setting. The ease and control in a laboratory setting are compelling motivations for performing acoustic measurements at the Acoustic Pressure Tank Facility (APTF). The acoustic measurements in this study were all conducted in the APTF. A cross-sectional diagram of the APTF is shown on the next page in Figure 29.

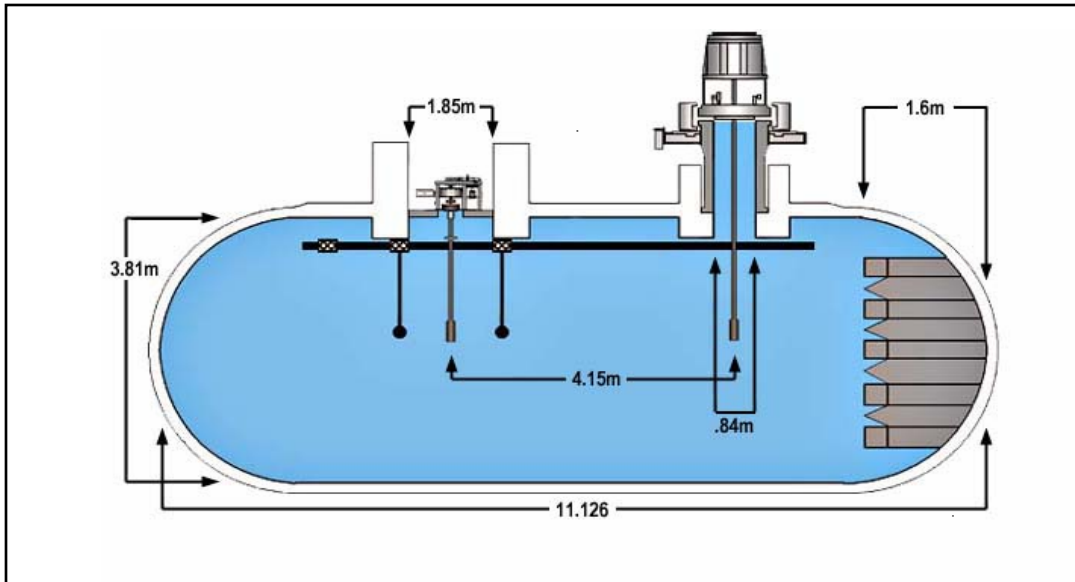


Figure 29. Cross-sectional diagram of the APTF<sup>14</sup>

The internal size of the tank (3.81 meters diameter x 11.126 meters long), combined with one end of the tank covered with an acoustic absorber to minimize reflections, augment the lower frequency range measurement capability. The thick walls (approximately 0.5 meter or 1.5 feet thick in some places) of the tank allow for high hydrostatic pressure acoustical testing in a controlled laboratory environment.

Capability to control environmental conditions makes the APTF unique. The temperature control of the water volume may be varied from 2°C to 35°C and hydrostatic pressures ranging from ambient pressure (at ~ 1.0 meter of depth) up to 18.6 MPa (2,700 psi, or ~ 1800 meters of depth). The inner volume of the tank holds approximately 30,000 gallons of fresh water and weighs just over one million pounds when filled [34]. Additional to the size that helps provide an environment for acoustically testing at low frequencies, one end of the tank is covered with acoustically absorbent wedges made of insulcrete, a material made from a mixture of sawdust and concrete (seen end-on in Figure 30). Insulcrete wedges, coupled with signal gating, averaging, and other signal processing techniques available to the measurement system operator permit a low

<sup>14</sup> Courtesy of Mr. Tony Paolero, Measurements Engineer and Facility Manager at the USRD

frequency test limit of electroacoustic transducers to as low as 1.0 kHz. Without special rigging to ensure measurements are performed on the main response axis (MRA), the upper frequency limit is 250 kHz.

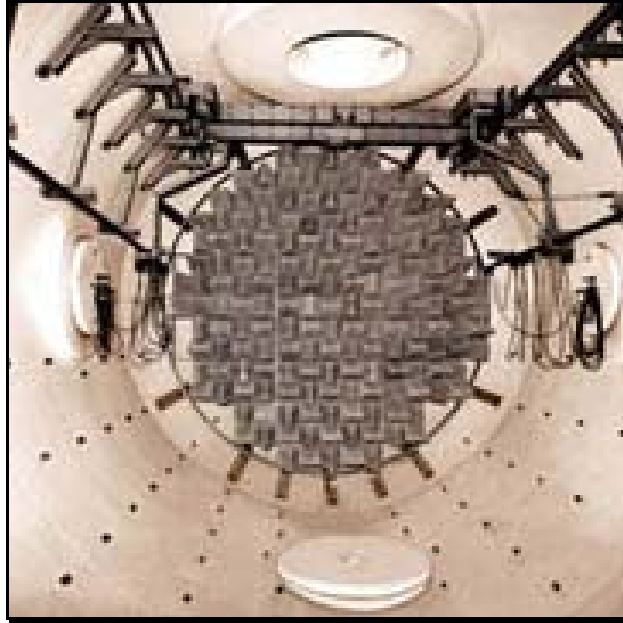


Figure 30. End view of insulcrete wedges at one end of the APTF<sup>15</sup>

---

<sup>15</sup> Courtesy of Mr. Tony Paolero, Acoustic measurements engineer and APTF facility manager

THIS PAGE INTENTIONALLY LEFT BLANK

## **VI. ACOUSTIC CYMBAL CONFIGURATIONS & TEST RESULTS**

Various design configurations of acoustic cymbal elements with passive pressure compensation approaches were fabricated and tested to determine transduction performance as a function of hydrostatic pressure. Each configuration is described and test results are provided.

### **A. PRESSURE COMPENSATION FOR UNDERWATER TRANSDUCERS**

A properly designed compensation system for an underwater transducer maintains a balance of equal pressure across the compliant components of a transducer so the maximum mechanical dynamic range can be fully utilized for converting acoustic energy to electrical energy or vice versa. A pressure compensation system should be used for a transducer (or single transducer element) when hydrostatic pressure in the application will otherwise mechanically clamp compliant components that are needed for energy conversion. Without one, hydrostatic pressure causes a pressure differential between the inside and the outside so consistent and/or effective performance is compromised. The obvious requirement for watertight integrity to protect the internal components results in compliant components on the inside being exposed to atmospheric pressure while the same compliant components, on the outside, are exposed to the elevated pressure generated by deep water. That pressure differential across the compliant components can cause a mechanical debilitation of the transduction process. Pressure compensation systems for underwater transducers can be either passive or active. Whether active or passive, some type of pressure compensation scheme is necessary for transducers with compliant components so consistent performance characteristics are maintained, especially if the environmental applications include deep water operations and hence, relatively high hydrostatic pressure.

#### **1. Passive Pressure Compensation Systems**

Passive compensation is preferred whenever possible because of its inherent simplicity and high reliability. One type of passive pressure compensation for moving coil transducers (Navy Standard J-series) utilizes a collapsible rubber bladder that

encloses the back side of the magnet/coil assembly [35]. When submersed, this rubber bladder is exposed to the hydrostatic pressure which causes it to collapse. On the other side (piston face), the compliant piston assembly is exposed to the same hydrostatic pressure but is balanced by equivalent pressures on both ends. This hydrostatic balance keeps the piston centered in the magnet assembly and performing optimally.

## **2. Active Pressure Compensation Systems**

Active compensation systems are more complex because of the requirement for an activating mechanism designed for consistency and reliability, a task that normally requires an iterative process of optimization. Additionally, the active system itself can be expensive and sizeable in relation to the transducer element itself. Active pressure compensation systems require some sort of stored energy, such as pressurized air, to provide a balance of hydrostatic pressure across the compliant components. One type of active pressure compensation, used for moving coil transducers (Navy Standard J-series), utilizes a smaller collapsible rubber bladder, but has a SCUBA tank strapped to the side to provide pressurized air. The second stage regulator of the SCUBA system is activated by a precisely positioned Schrader valve [35]. As depth increases, the Schrader valve is activated, allowing the proper volume of compressed gas to push the piston head back into the preferred position. Active compensation systems are not recommended for relatively small devices.

## **3. Pressure Testing**

Methods employed to evaluate the hydrostatic response of a device are not always determined during an acoustic measurement in water. Professor Robert Newnham and his team of researchers at The Pennsylvania State University use a pressure chamber to determine the change, as it relates to a side-by-side measurement to a standard, in hydrostatic piezoelectric voltage constant ( $g_h$ ) to predict performance differences [10]. However, the most assured method of testing acoustic performance at varied hydrostatic pressure is to actually measure the performance under a controlled environment. This can be accomplished in the APTF at NUWC Newport.



## **B. NAVY ACOUSTIC CYMBAL ELEMENT “STANDARD”**

One type of acoustic cymbal element recently featured in other applications is a Navy design, which this author established early on to be the foundational standard for this investigation. This design does not have any inherent pressure compensation system as, to date, it has only been used for shallow water applications. The configuration of this standard has a small (0-80) threaded stud welded perpendicular to the apex center surface on each of the two radiating shells (as seen in Figure 31).



Figure 31. Navy acoustic cymbal element ‘standard’ design

A key purpose in having the threaded post is to establish both electrical and mechanical connections. Mechanically, the post is affixed to a stiff plate that functions as an acoustic radiation diaphragm. Furthermore, small nuts can be added to lower the fundamental frequency (by virtue of the added weight) of the individual sensor to enhanced desired low frequency performance [33].

Three of these cymbal element standards were tested to determine the consistency of performance that might be gained by adhering to stringent manufacturing procedures. Table 3 shows the FFVS and TVR performance characterization tests at variable hydrostatic pressures for three standard cymbal elements.

Table 3. Test Matrix for Cymbal Element Standards

Pressure	Pressure	Depth	STD#1		STD#2		STD#3	
(kPa)	(psi)	(ft.)	FFVS	TVR	FFVS	TVR	FFVS	TVR
28	4	9	2104-33	2104-45	2104-49	2104-61	2104-65	2104-77
345	50	110	“	“	“	“	“	“
690	100	219	“	“	“	“	“	“
1379	200	439	“	“	“	“	“	“
1724	250	548						
2069	300	658	2104-34	2104-46	2104-50	2104-62	2104-66	2104-78
2758	400	877	“	“	“	“	“	“
3103	450	987	“	“	“	“	“	“
3448	500	1097	“	“	“	“	“	“
4137	600	1316	2104-35	2104-47	2104-51	2104-63	2104-67	2104-79
4827	700	1535	“	“	“	“	“	“
5171	750	1645						
6895	1000	2193						
8619	1250	2741						
3448*			“	“	“	“	“	“
28**			2104-36	2104-48	2104-52	2104-64	2104-68	2104-80

\* Repeated, \*\* Before and after pressurization comparison

Given that the acoustic data is comparatively consistent between individual cymbal elements tested, FFVS and TVR data for only one of these Navy Standards is shown in Figures 32 and 33 respectively. FFVS shows the fundamental resonance frequency is located consistently at slightly less than 15 kHz yet begins to dampen at 500 psi. Six out of the 12 acoustic measurements that were performed at specific hydrostatic pressures (reference Table 3 above), established both consistency of the acoustic cymbal performance at increasing pressures and how performance is altered by higher pressures. Ambient pressure (approximately 4 psi) is used as the baseline for both performance parameters. Performance was surprisingly consistent from one element to another until a pressure of about 500 psi was reached. By 600 psi both FFVS and TVR performance had changed substantially. The data substantiates claims that the standard acoustic cymbal can behave consistently to pressures up to 500 psi, which corresponds to nearly 335 meters (or ~1100 feet) of depth in seawater.

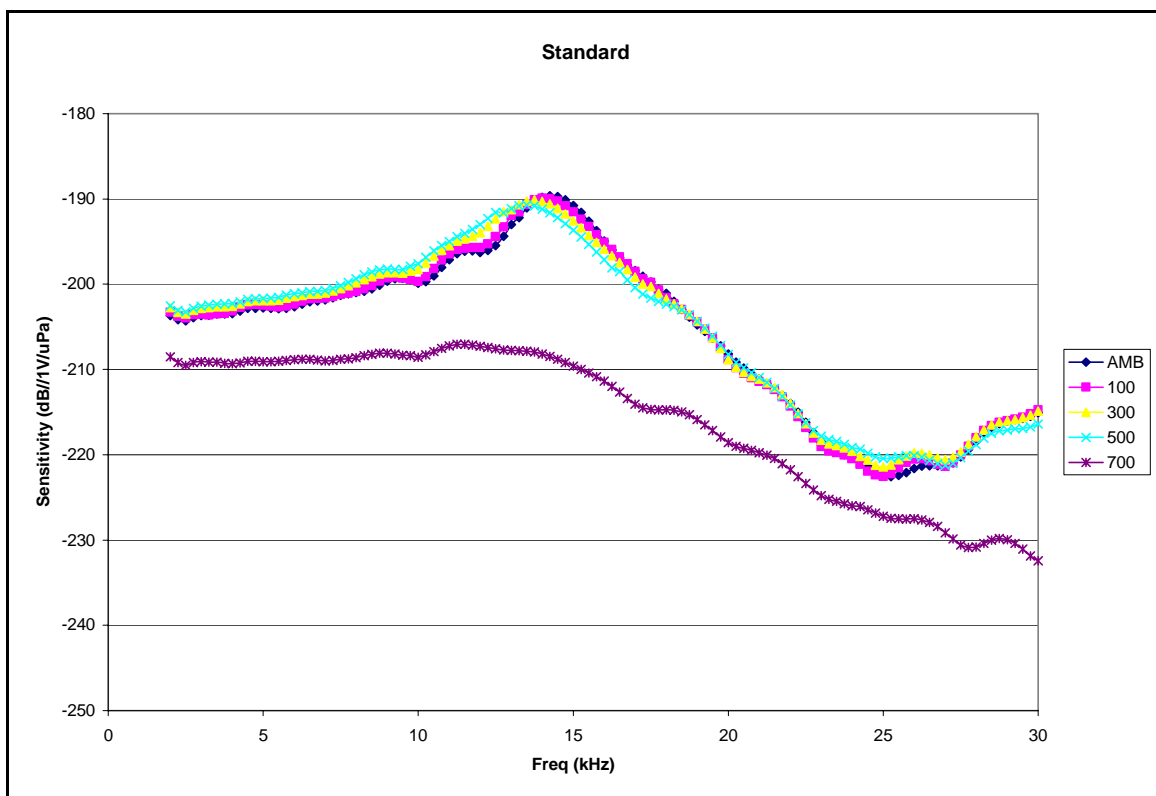


Figure 32. FFVS of cymbal element standard at varying pressures (psi)

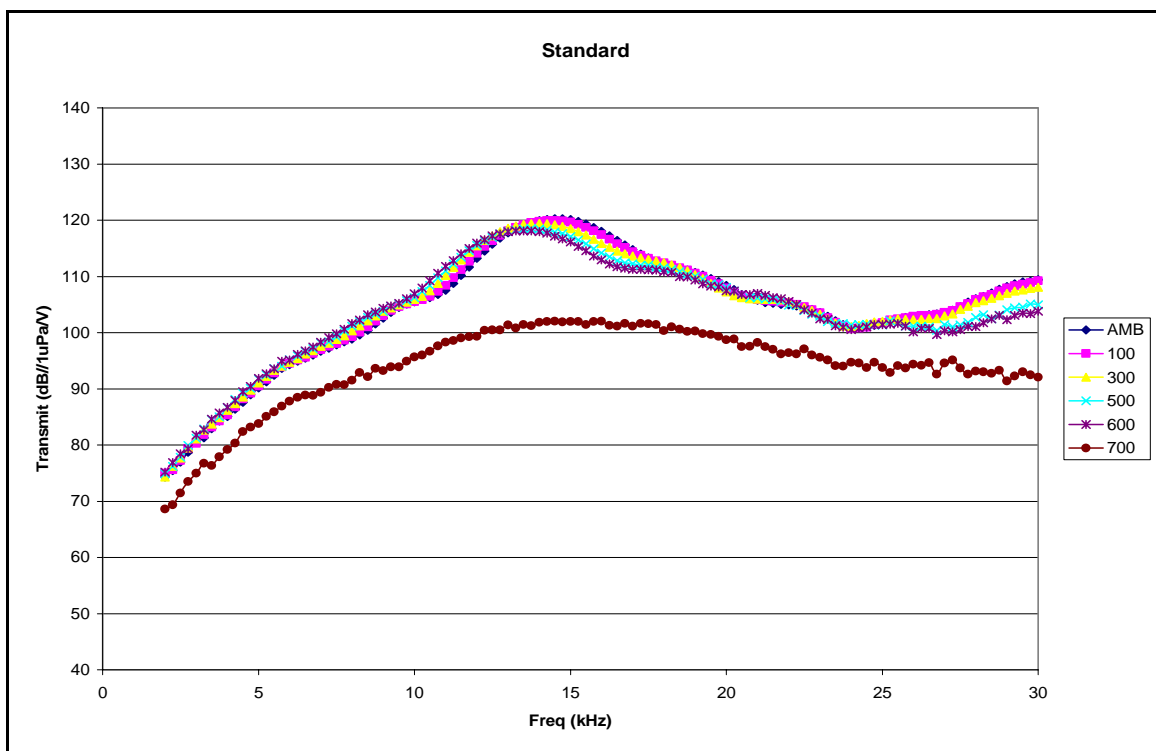


Figure 33. TVR of cymbal element standard at varying pressures (psi)

### C. INVERTED RING SHELLS OR “DOUBLE-DIPPERS”

A distinctive style of cymbal element that was tested is a class VII flextensional transducer called the “double-dipper” configuration. Like the original acoustic cymbal element, the relatively new double-dipper configuration was conceived by a Materials Research Laboratory (MRL) team guided by Professor Robert E. Newnham at The Pennsylvania State University [10]. The configuration of the double-dipper is different in that the cymbal shell is concave as opposed to convex. In order to accommodate this concave configuration, the piezoceramic actuator is a ring instead of a disk. The ring makes allowance for the cymbal shell to flex in and out of the center hole without interference. The idea behind the double-dipper is that decreased volume between the radiating cymbal shells might diminish the depth dependence. Table 4 shows the FFVS and TVR performance characterization tests at variable hydrostatic pressures for two double-dipper cymbal elements.

Table 4. Test Matrix for Double-Dipper Cymbal Elements

Pressure (kPa)	Pressure (psi)	Depth (ft.)	1mm thk FFVS	TVR	3mm thk FFVS	TVR
28	4	9	2104-17	2104-10	2169-1	2169-10
345	50	110	“	“		
690	100	219	“	“	“	“
1379	200	439	“	“		
1724	250	548			“	“
2069	300	658	2104-18	2104-30		
2758	400	877	“	“		
3103	450	987	“	“		
3448	500	1097	“	“	“	“
4137	600	1316	2104-19	2104-31		
4827	700	1535				
5171	750	1645			“	“
6895	1000	2193			2169-2	2169-11
8619	1250	2741			“	“
3448*			“	“		
28**			2104-20	2104-32	2169-3	2169-12

\* Repeated, \*\* Before and after pressurization comparison

## 1. One mm Thick Driver Element

The first double-dipper tested uses a one mm thick piezoceramic ring as the drive element. FFVS and TVR measurements displayed in Figures 36 and 37 respectively show that resonances shifted upwards as the pressure was increased so that by 400 psi, the acoustic performance was deemed inconsistent with respect to hydrostatic pressure.

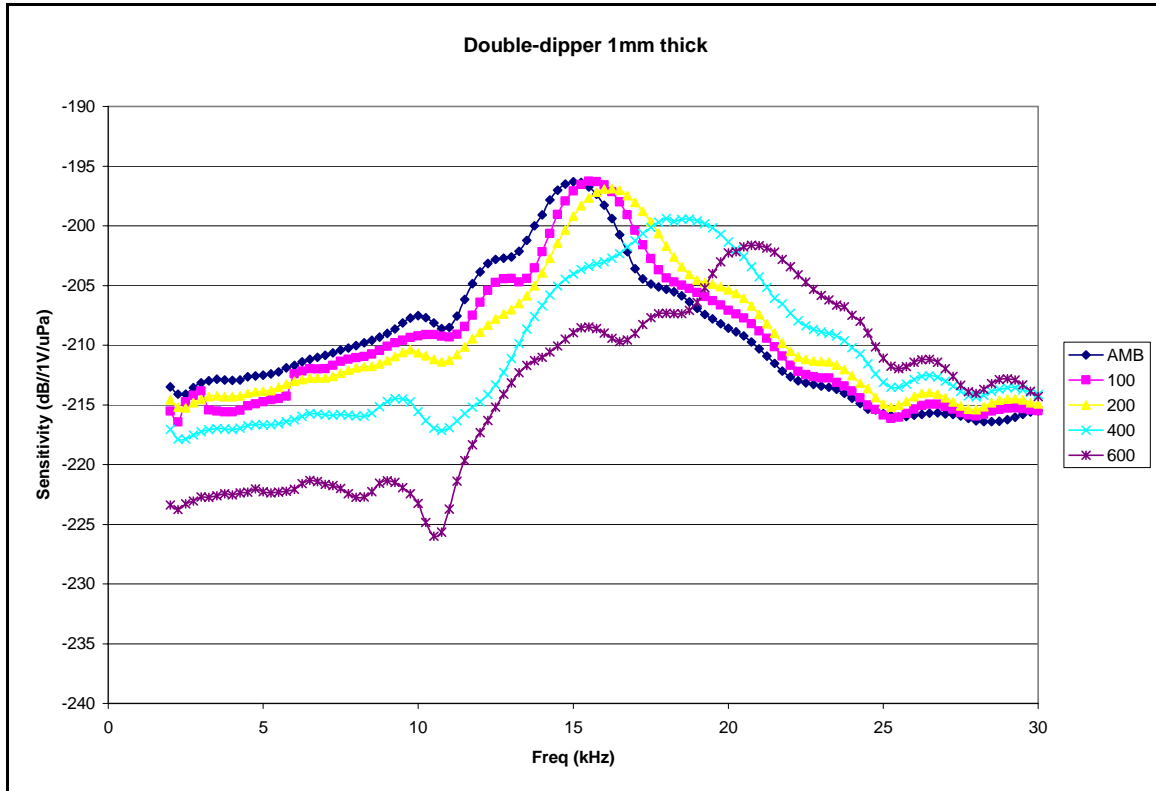


Figure 34. FFVS of double-dipper (1mm thick) at varying pressures (psi)

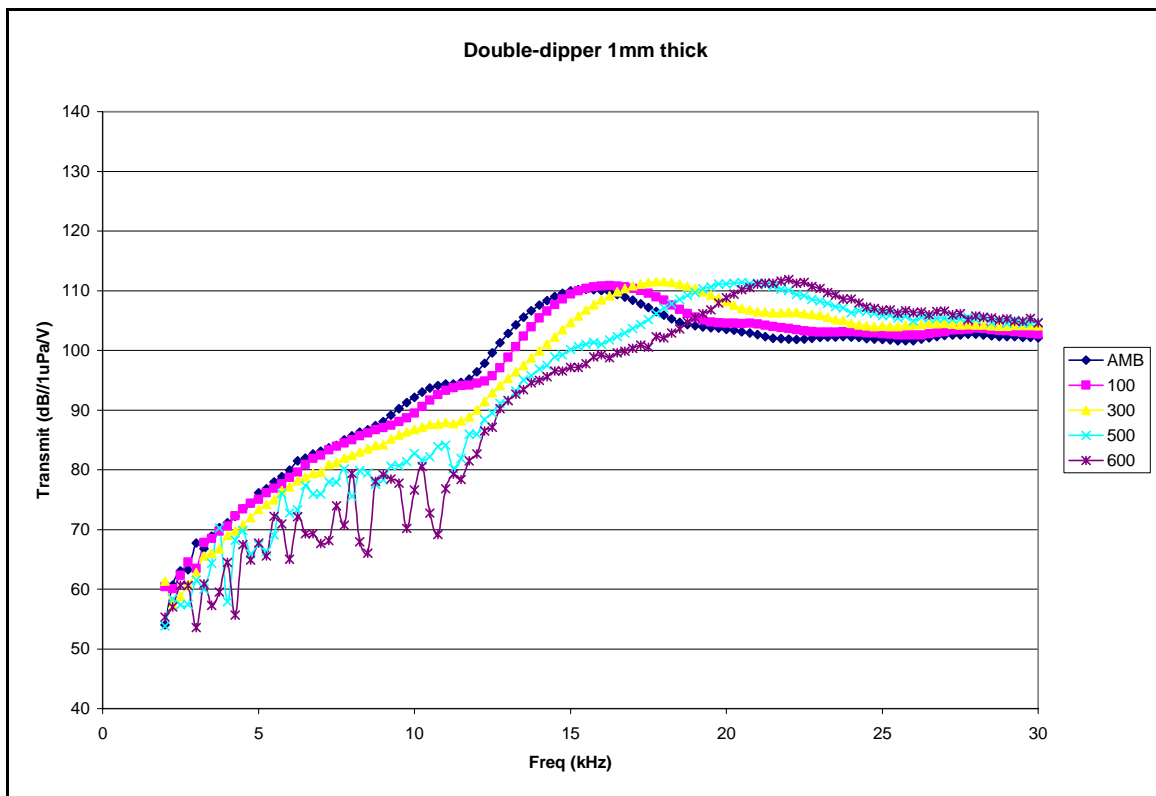


Figure 35. TVR of double-dipper (1mm thick) at varying pressures (psi)

## 2. Three Millimeter Thickness

The second double-dipper tested uses a three mm thick piezoceramic ring as the drive element. Extreme variability in performance with respect to changes in hydrostatic pressure was measured and is shown in Figures 36 and 37. The performance was significantly inconsistent even from ambient pressure to 250 psi. The resonances shifted upwards as the pressure was increased so that by 500 psi, the acoustic performance was obviously inconsistent. Without significant change in the design, this style of transducer is not adequate for use in Navy systems required to operate consistently in a wide range of hydrostatic pressures.

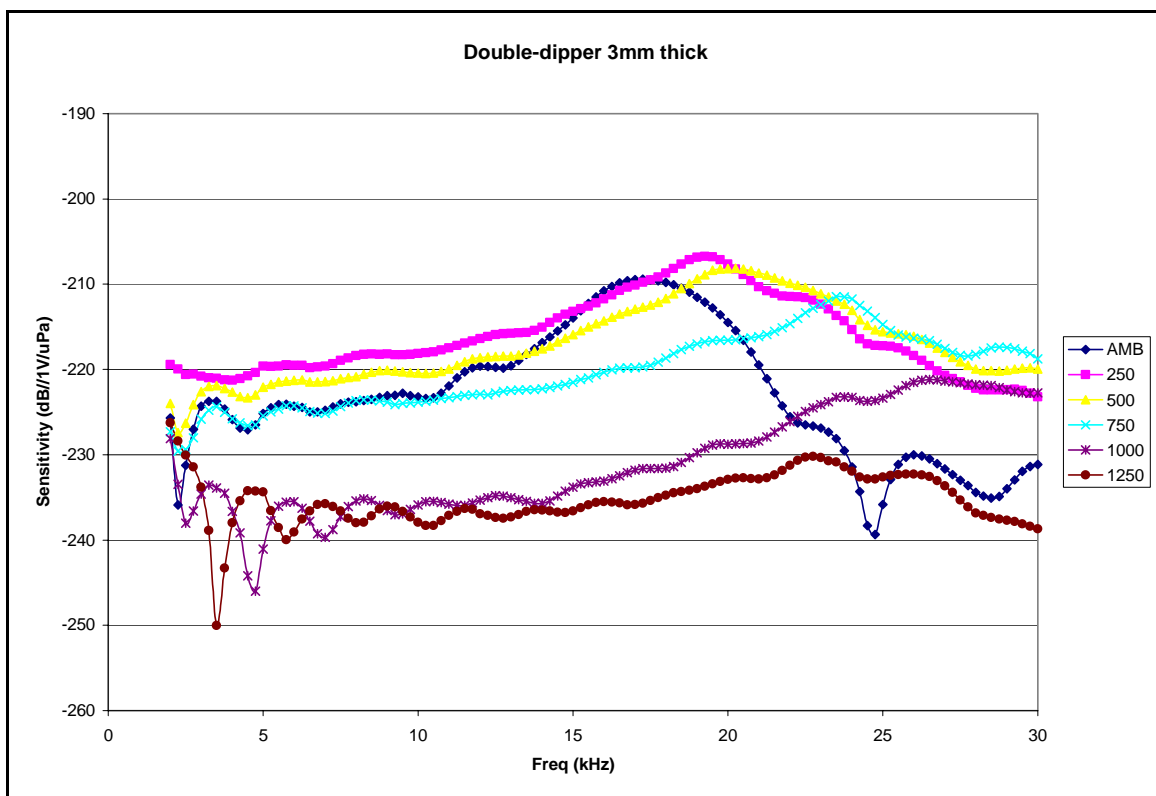


Figure 36. FFVS of double-dipper (3mm thick) at varying pressures (psi)

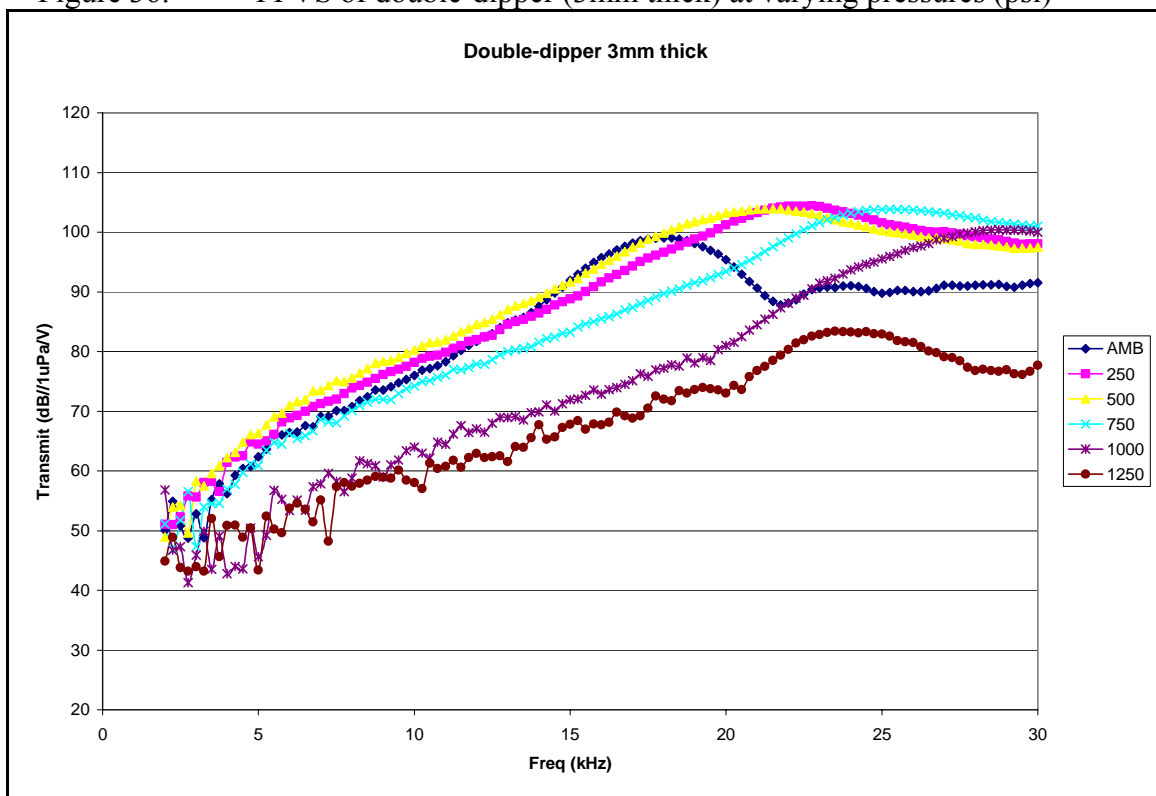


Figure 37. TVR of double-dipper (3mm thick) at varying pressures (psi)

#### D. CYMBAL ELEMENTS OF VARYING SHELL DEPTHS

Still another alternative type of cymbal element tested has shell depths deeper than the standard. The cymbal shell itself is attached in the same manner to the piezoceramic driver as the standard except that it does not have the threaded post welded to the apex. It is notable that the greater heights of the flexural shell approximate a spherical shape, the optimal configuration for resisting hydrostatic pressure, but an unknown variable when used as part of a cymbal element. However, it is expected that this type will have less effective FFVS and TVR. For lack of better terms, these types are named by using numbers associated with the depth (in microns) of the radiating shell. Table 5 shows the FFVS and TVR performance characterization tests at variable hydrostatic pressures for two cymbal elements labeled type 600 and type 900.

Table 5. Test Matrix for Cymbal Elements of varying heights

Pressure	Pressure	Depth	Type 600		Type 900	
(kPa)	(psi)	(ft.)	FFVS	TVR	FFVS	TVR
28	4	9	2104-17	2104-10	2169-1	2169-10
345	50	110	“	“		
690	100	219	“	“	“	“
1379	200	439	“	“		
1724	250	548			“	“
2069	300	658	2104-18	2104-30		
2758	400	877	“	“		
3103	450	987	“	“		
3448	500	1097	“	“	“	“
4137	600	1316	2104-19	2104-31		
4827	700	1535				
5171	750	1645			“	“
6895	1000	2193			2169-2	2169-11
8619	1250	2741			“	“
3448*			“	“		
28**			2104-20	2104-32	2169-3	2169-12

\* Repeated, \*\* Before and after pressurization comparison

##### 1. Type 600

The type 600 has a shell depth of approximately 600 microns (0.6 mm or 0.0236 inch). As seen by the FFVS and TVR data in Figures 38 and 39, this design does not perform in a stable manner as hydrostatic pressure is applied. In part of the band of



interest (approximately 20 kHz), the FFVS dropped more than 30 dB as the pressure was increased from ambient to 250 psi. Correspondingly, the TVR dropped nearly 40 dB. Though the rationale for this inconsistent performance is uncertain, it is speculated that the hydrostatic pressure collapsed the relatively larger inner volume and stiffened the shell in a way that the piezoelectric effectiveness for transmitting and receiving were compromised. Without significant change in the design, this style of transducer is not adequate for use in Navy systems required to operate consistently in a wide range of hydrostatic pressures.

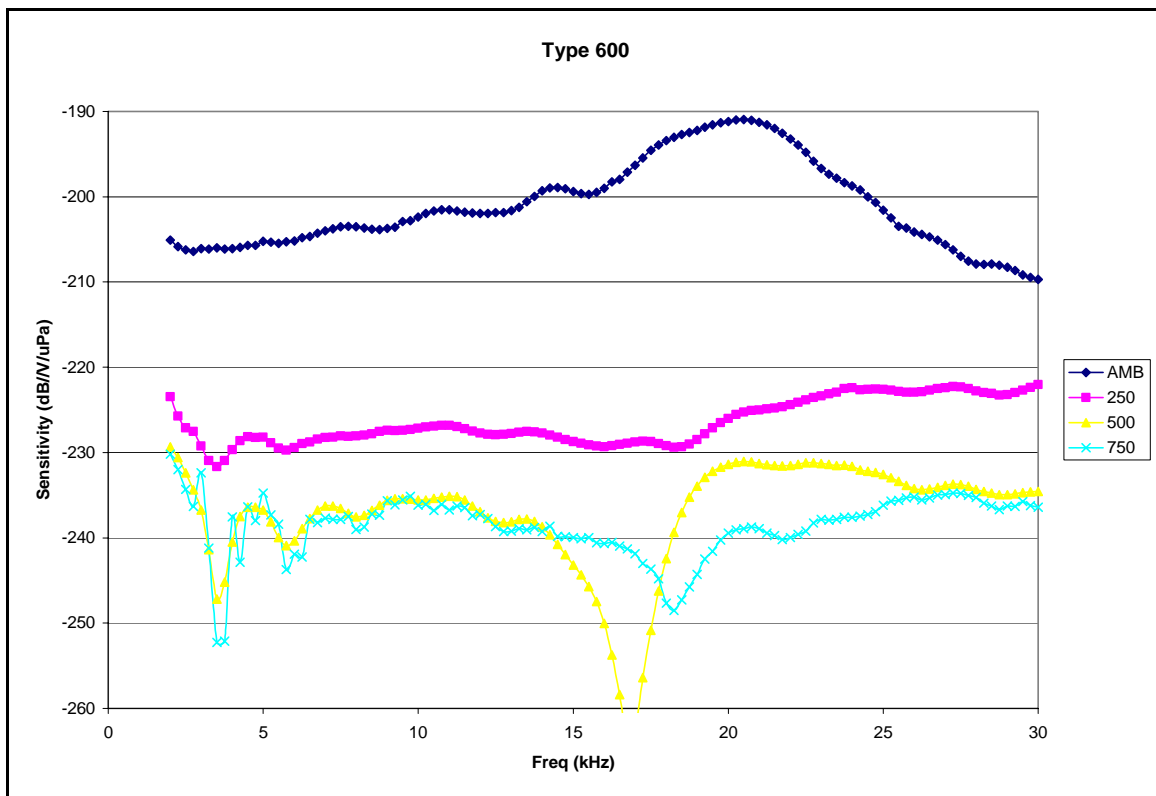


Figure 38. FFVS of cymbal element type 600 at varying pressures (psi)

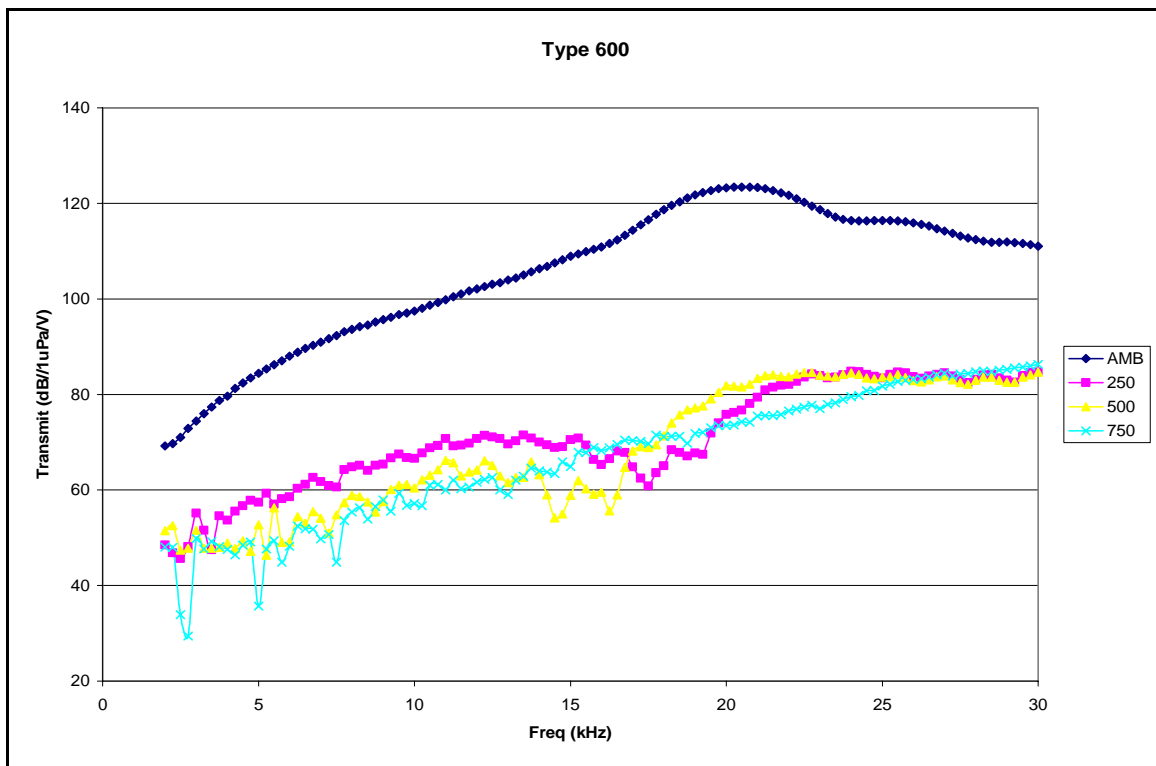


Figure 39. TVR of cymbal element type 600 at varying pressures (psi)

## 2. Type 900

The type 900 has a shell depth of approximately 900 microns (0.9 mm or 0.0354 inch). As seen by the FFVS and TVR data in Figures 40 and 41, this design also does not perform in a stable manner as hydrostatic pressure is applied. In part of the band of interest (approximately 20 kHz), the FFVS was altered as the pressure increased from ambient to 250 psi. And differently from the type 600, the FFVS drops instead only 20 dB when the pressure is increased from 250 psi to 500 psi. Correspondingly, the TVR also dropped approximately 20 dB. The inconsistency in performance for Type 900 could possibly be attributed to the same problem as Type 600 with the same uncertainty; hydrostatic pressure collapsed the relatively larger inner volume and stiffened the shell such that the piezoelectric effectiveness for transmitting and receiving were compromised. Apparently though, the difference was lessened by the deeper shell. Without significant change in the design, this style of transducer is not adequate for use in Navy systems required to operate consistently in a wide range of hydrostatic pressures.

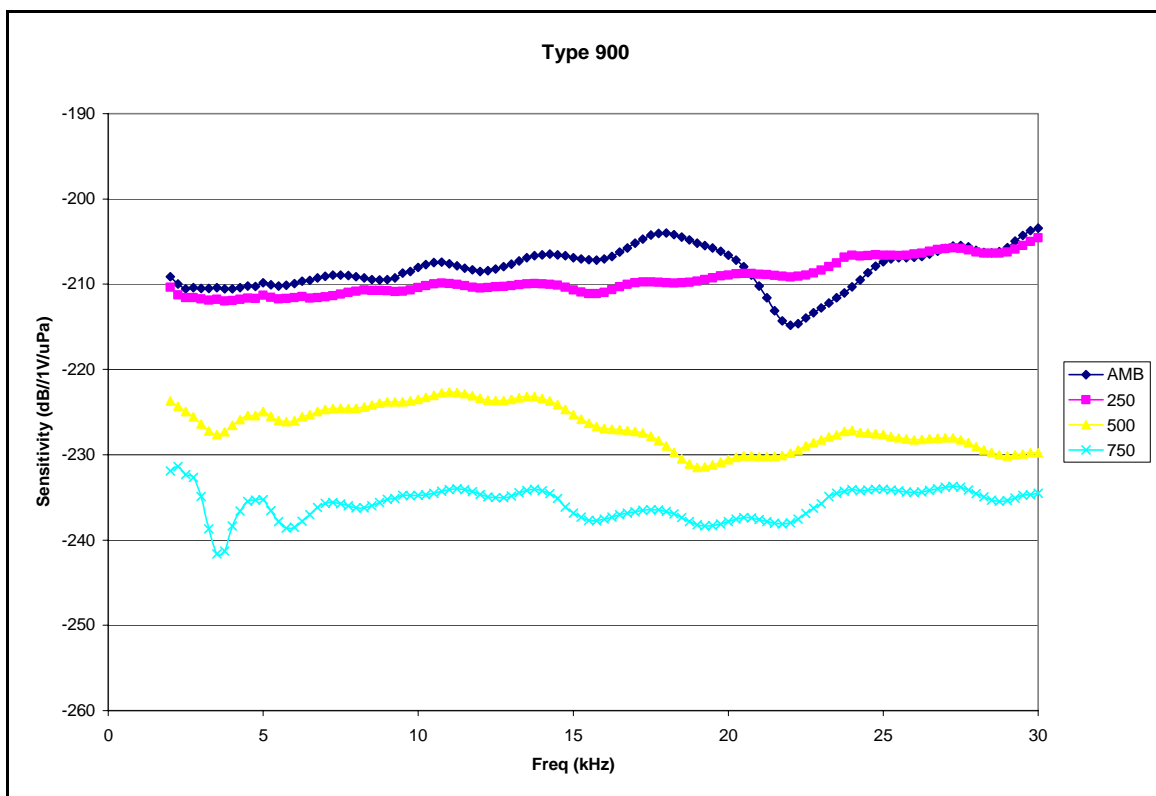


Figure 40. FFVS of cymbal element type 900 at varying pressures (psi)

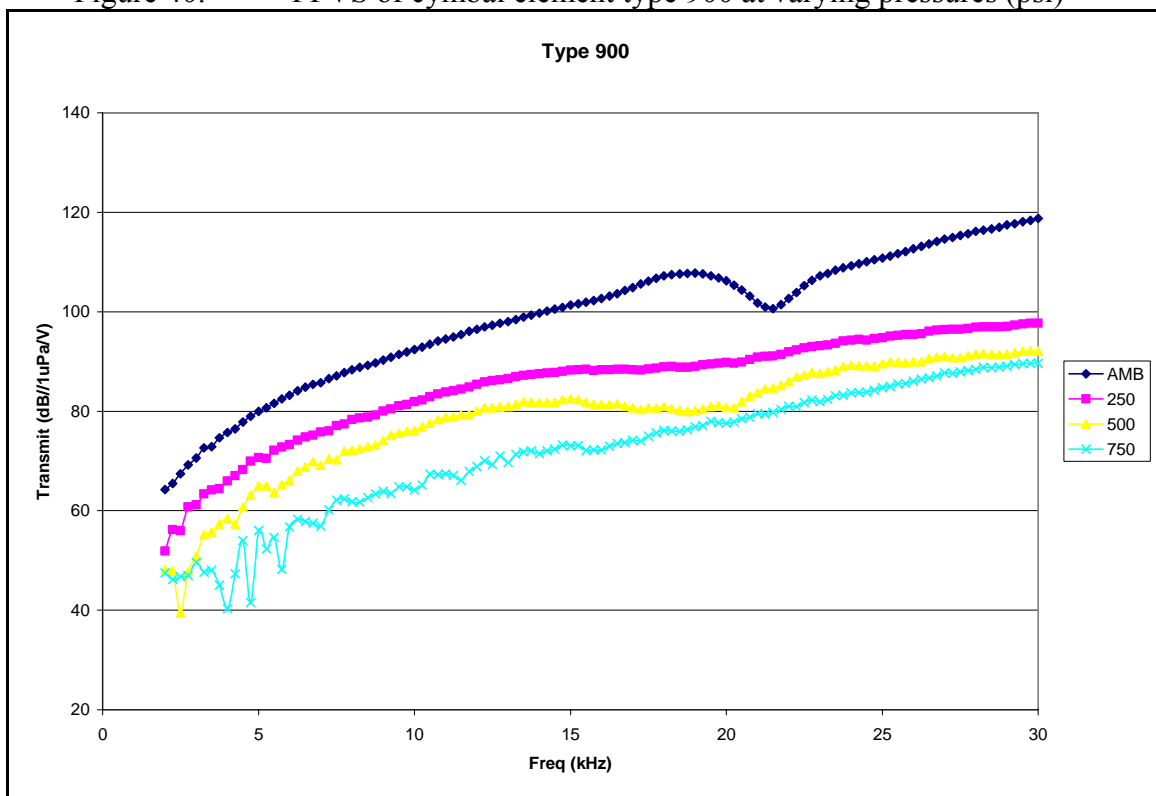


Figure 41. TVR of cymbal element type 900 at varying pressures (psi)

## **E. ACOUSTIC CYMBAL ELEMENTS WITH PORTS**

Modified versions of the cymbal element standard are ones that have ports of different sizes and configurations drilled through the flexural shell itself, prior to bonding to the piezoceramic disk, in a symmetric manner (3 holes in each shell, 120° apart). The ports allow the fill fluid (evacuated castor oil) to flow behind the cymbal shell in order to establish a balance of pressure across the cymbal shells. A hole in the flexing shell is considered passive compensation.

### **1. Holes Near the Apex (Apex Holes)**

The first attempt at this type of passive pressure compensation design had holes drilled near the apex to allow the backside of the shell to be free-flooded with castor oil. Each hole for this version is 0.039 inch (1mm) in diameter and the edge of each hole was tangent to the outside edge of the apex as shown in Figure 42. In the foreground are a washer and nut used to mechanically affix the flexible copper electrical conductor strips. Table 6 shows the FFVS and TVR performance characterization tests at variable hydrostatic pressures for a cymbal element with holes near the apex.

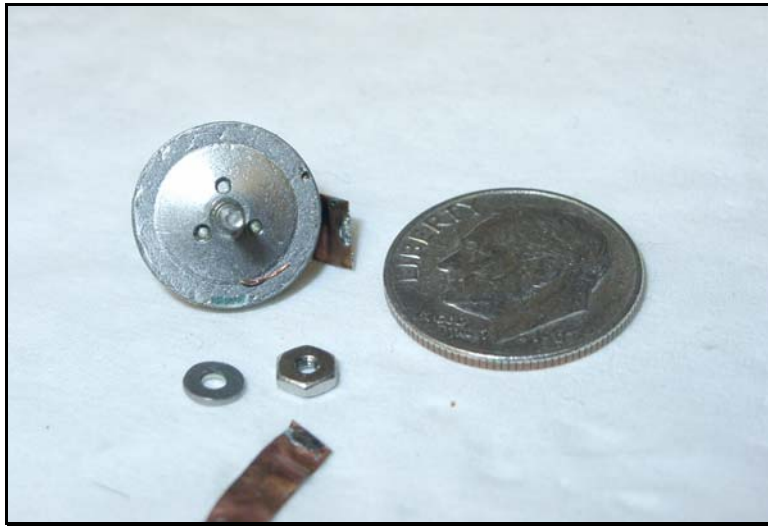


Figure 42. Cymbal elements with holes near the apex

Table 6. Test Matrix for Cymbal Element with Holes Near Apex

Pressure	Pressure		Apex Holes	
(kPa)	(psi)	Depth	FFVS	TVR
28	4	9	2104-1	2104-13
345	50	110	“	“
690	100	219	“	“
1379	200	439	“	“
1724	250	548		
2069	300	658	2104-2	2104-14
2758	400	877	“	“
3103	450	987	“	“
3448	500	1097	“	“
4137	600	1316	2104-3	2104-15
4827	700	1535	“	“
5171	750	1645		
6895	1000	2193		
8619	1250	2741		
3448*			“	“
28**			2104-4	2104-16

\* Repeated, \*\* Before and after pressurization comparison

FFVS and TVR data for the cymbal element with apex holes are shown in Figures 43 and 44. Both the FFVS and TVR data for this cymbal element remains fairly consistent from the low frequency to the fundamental resonance with respect to hydrostatic pressure until about 500 psi. Somewhere between 500 psi and 700 psi consistency of the performance in both measurement modes drops significantly. At about 14 kHz, the FFVS drops 15 dB and TVR shows erratic performance. Some of this erratic performance in TVR can be attributed to the fact that some elements inside the platform that were being tested simultaneously with this cymbal element had failed and introduced air in the castor oil. The air in the castor oil functions as a pressure release in the acoustic field that corrupts performance measurements.

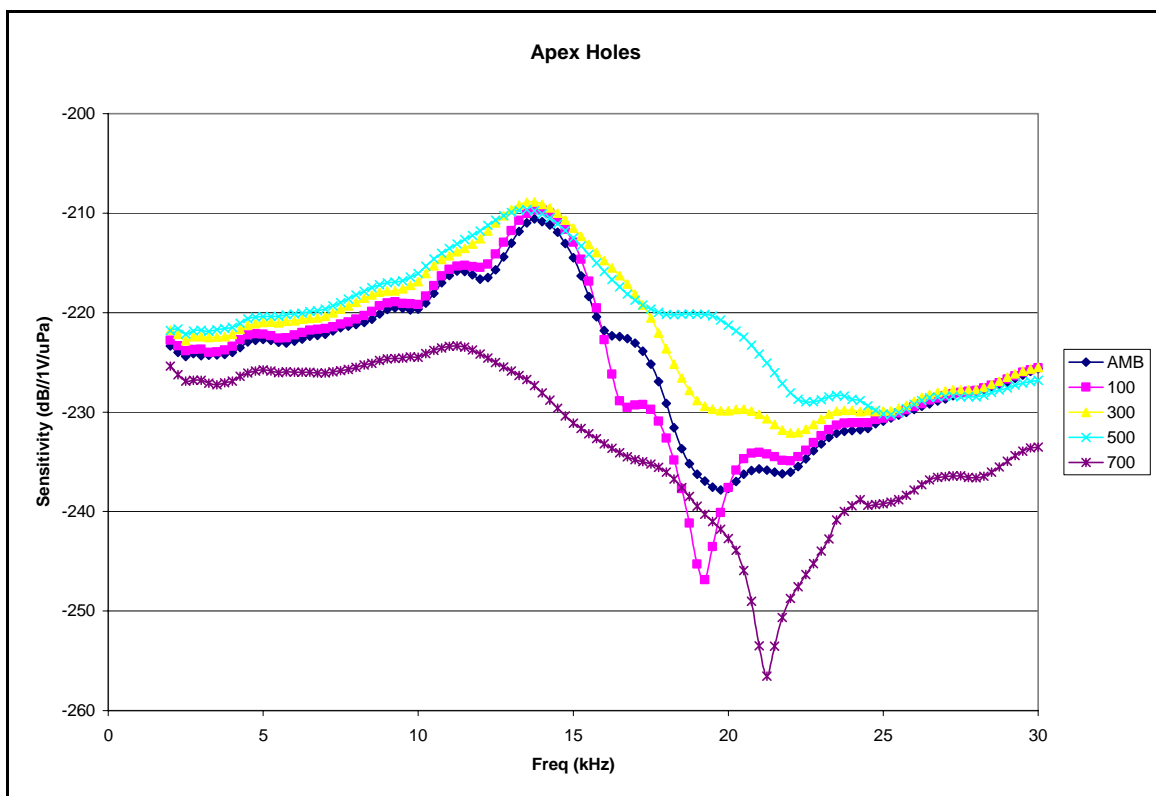


Figure 43. FFVS of cymbal element with apex holes at varying pressures (psi)

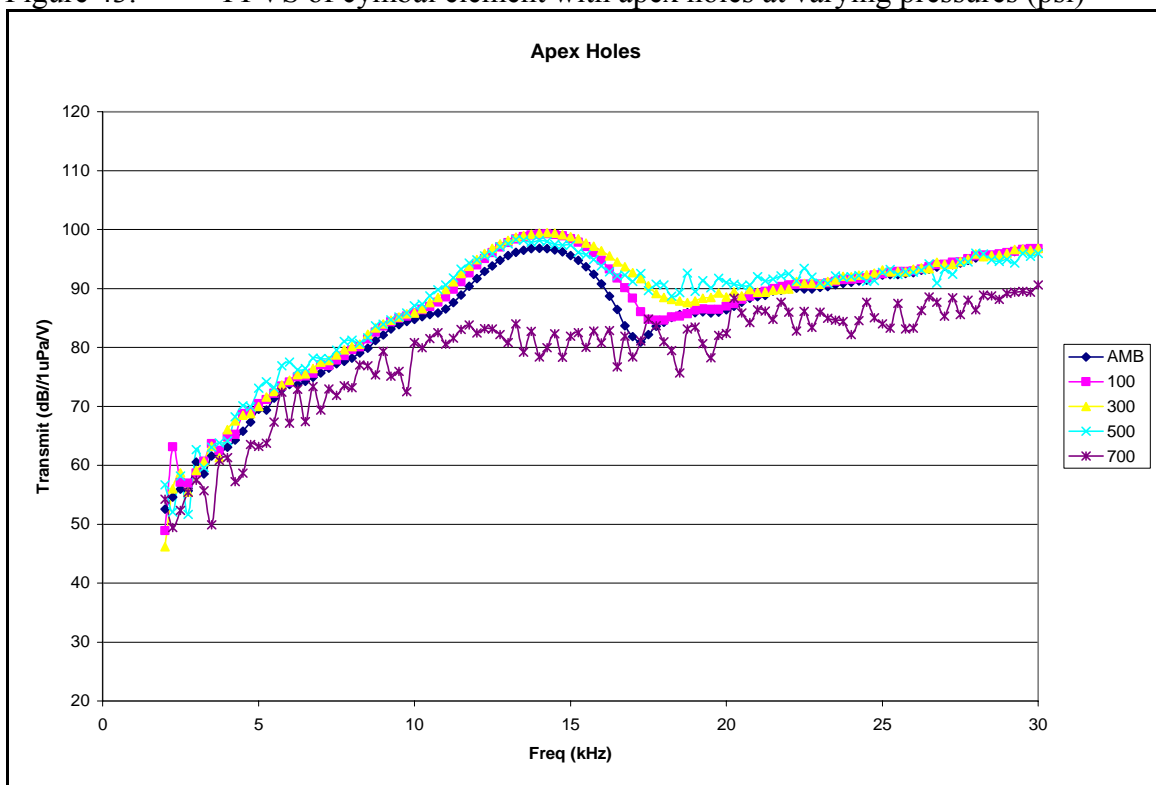


Figure 44. TVR of cymbal element with apex holes at varying pressures (psi)

## 2. Shells with Slots

Based on the measurements from cymbal elements with apex holes, slots were considered. Three slots (0.020" W x 0.073" L) were machined into each radiating shell as shown in Figure 45. The intent was not only to maintain a balance of pressure across the surfaces but also to introduce increased flexibility in the radiating shell. Table 7 shows the list of FFVS and TVR performance characterization tests. Results for FFVS and TVR tests on the cymbal elements with slots are shown in Figures 48 and 49.



Figure 45. Cymbal element with Slots

Table 7. Test Matrix for Cymbal Elements with Slots

Pressure (kPa)	Pressure (psi)	Depth (ft.)	Slots#1 FFVS	TVR	Slots#2 FFVS	TVR
28	4	9	2228-25	2228-34	2228-37	2228-46
345	50	110				
690	100	219	"	"	"	"
1379	200	439				
1724	250	548	"	"	"	"
2069	300	658				
2758	400	877				
3103	450	987				
3448	500	1097	"	"	"	"
4137	600	1316				
4827	700	1535				
5171	750	1645	2228-26	2228-35	2228-38	2228-47
6895	1000	2193	"	"	"	"
8619	1250	2741	"	"	"	"
3448*						
28**			2228-27	2228-36	2228-39	2228-48

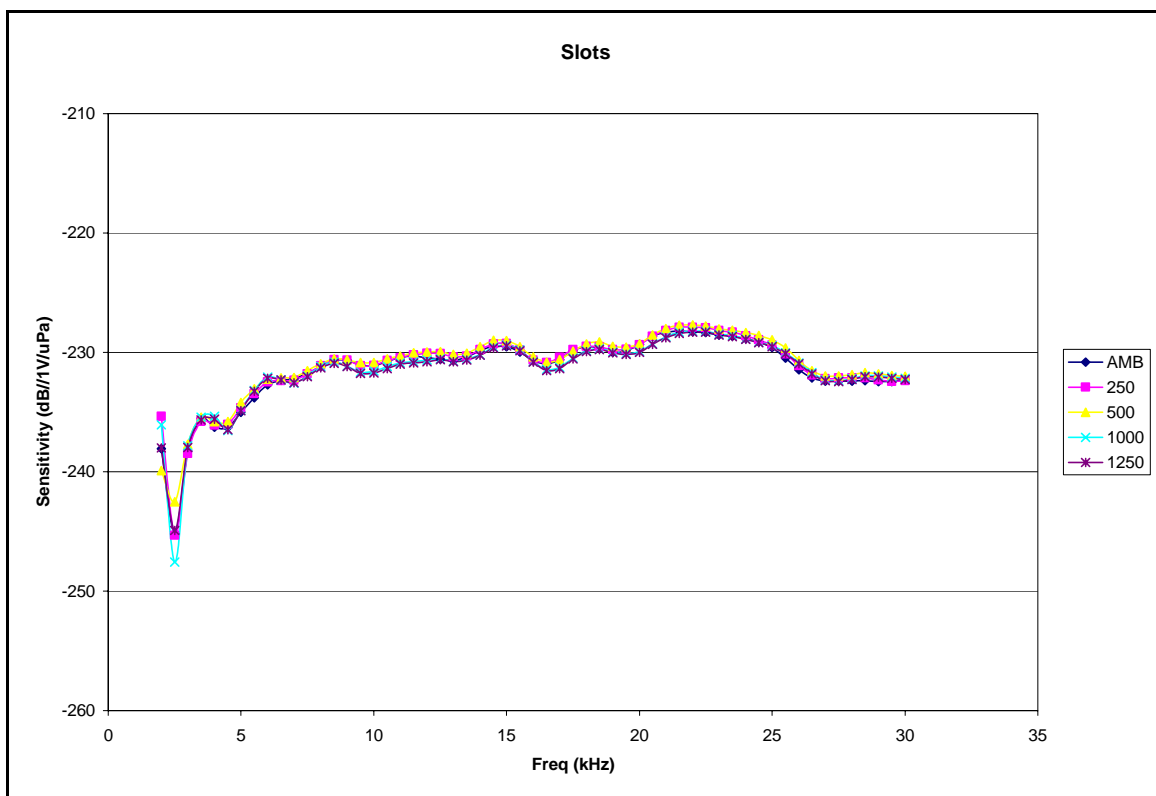


Figure 46. FFVS of cymbal element with slots at varying pressures (psi)

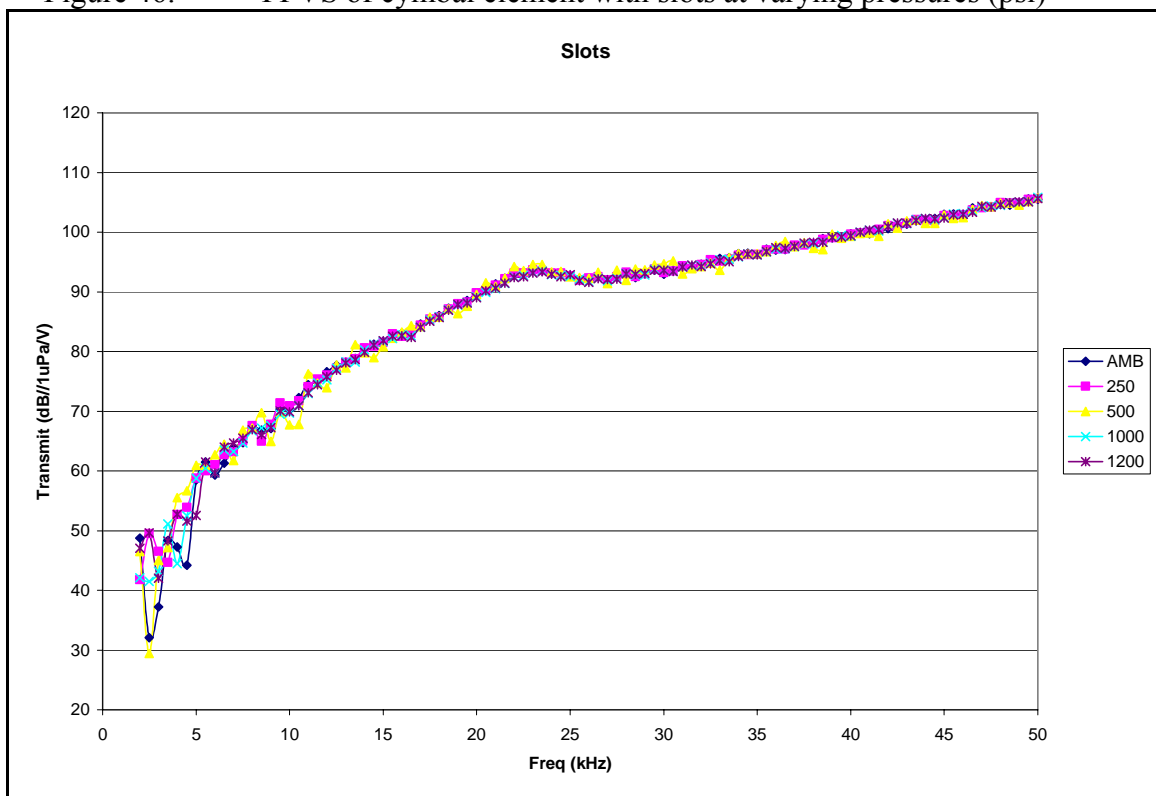


Figure 47. TVR of cymbal element with slots at varying pressures (psi)



The FFVS and TVR data show that the performance of this cymbal element is consistent across a wide band of interest. Because of the consistent performance with respect to hydrostatic pressure, this style of transducer may be adequate for use in Navy systems required to operate consistently in a wide range of hydrostatic pressures.

### **3. Small Holes at Outer Edge (Edge Holes)**

Considering results from the holes near the apex and the slots brought about thinking that acoustic performance might be improved if the holes were smaller and moved further away from the center. Figure 48 shows one of the two acoustic cymbals built with holes relocated as close as possible to the inside edge of the flange that is used for bonding to the piezoceramic. The holes were located far enough away from the inside edge such that the epoxy bead would not be an obstruction for oil to flow through the holes while the transducer was being filled with castor oil. The 0.015" diameter holes still allow the inside cavity to be filled with castor oil for pressure compensation, but the smaller size was intended to limit leakage of acoustic energy through the ports back to the inside surface of the radiating shells. Such leakage inhibits favorable performance at lower frequencies. Table 8 shows the FFVS and TVR performance characterization tests at variable hydrostatic pressures for two cymbal elements with small holes.



Figure 48. Cymbal element with very small holes near inner edge of flange

Table 8. Test Matrix for Cymbal Elements with Edge Holes

Pressure	Pressure	Depth	Edge#1		Edge#2	
(kPa)	(psi)	(ft.)	FFVS	TVR	FFVS	TVR
28	4	9	2228-1	2228-10	2228-13	2228-23
345	50	110				
690	100	219	“	“	“	“
1379	200	439				
1724	250	548	“	“	“	“
2069	300	658				
2758	400	877				
3103	450	987				
3448	500	1097	“	“	“	“
4137	600	1316				
4827	700	1535				
5171	750	1645	2228-2	2228-11	2228-14	2228-23
6895	1000	2193	“	“	“	“
8619	1250	2741	“	“	“	“
3448*						
28**			2228-3	2228-12	2228-15	2228-24

\*Repeated, \*\* Before and after pressurization comparison

As seen in Figures 49 and 50, the FFVS and TVR data show that the performance of this cymbal element is consistent across a wide band of interest. Because of the consistent performance with respect to hydrostatic pressure, this style of transducer may be adequate for use in Navy systems required to operate consistently in a wide range of hydrostatic pressures.

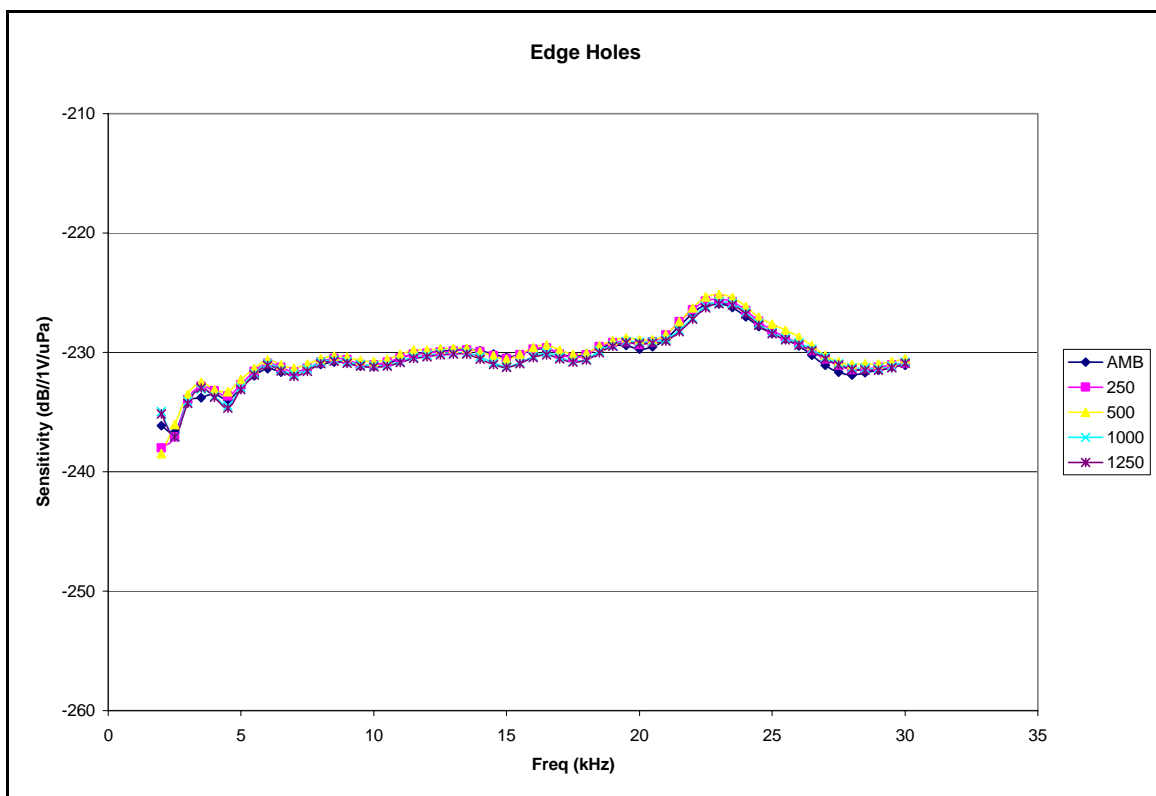


Figure 49. FFVS of cymbal element with edge holes at varying pressures (psi)

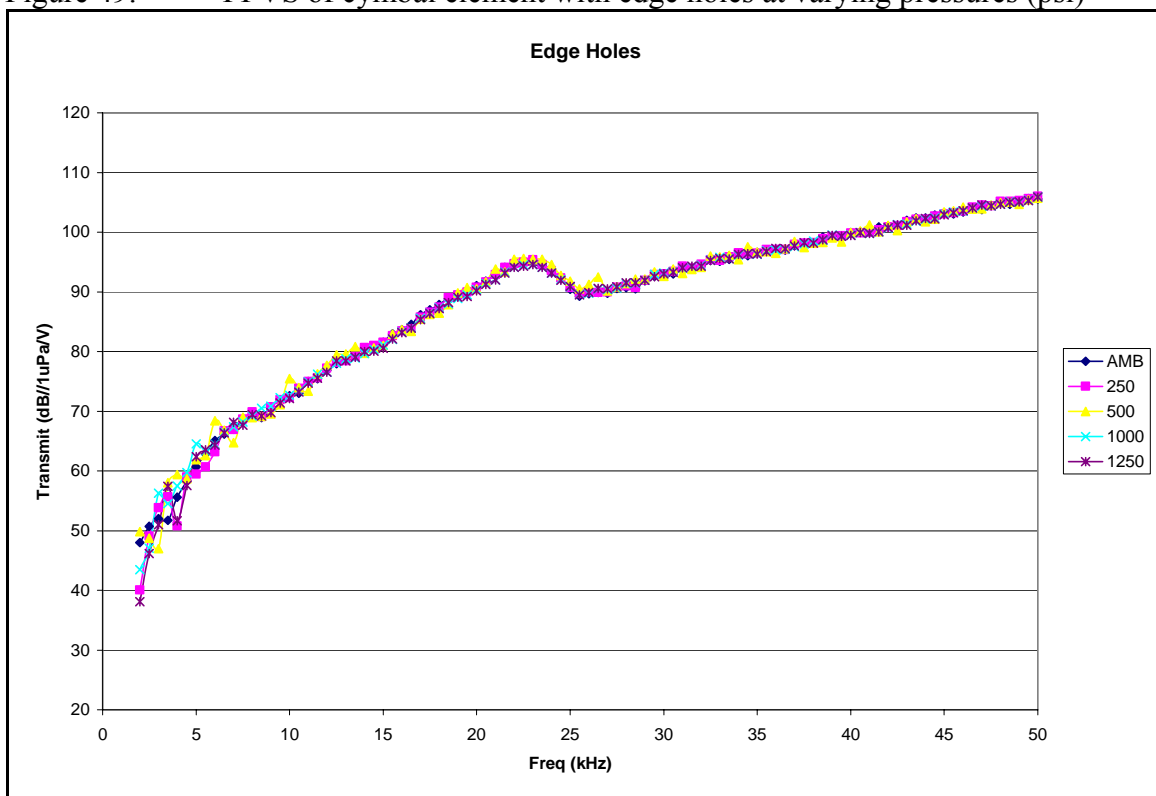


Figure 50. TVR of cymbal element with edge holes at varying pressures (psi)

## **F. ACOUSTIC MEASUREMENTS SUMMARIZED**

Measurements of the various cymbal element types revealed that some configurations performed better at higher hydrostatic pressures than others. Because the physics of performance for each type can only be surmised by limited observation through measurement, no recommendations about how to improve each type can be accurately made. The Navy acoustic cymbal standards performed very consistently within a restricted range of hydrostatic pressure (up to 600 psi).

Double-dipper cymbal elements showed high sensitivity near their resonances of 15 kHz and 20 kHz for the one millimeter thick ceramic and the three millimeter thick piezoceramics respectively. Acoustic measurements show that the double-dippers as they are currently configured are insufficient performers for applications involving variable hydrostatic pressure applications because of the irregularity of performance.

The two cymbal element Types 600 and 900 (deeper shells with respect to the standard) performed erratically with variable pressure. Nominal expectations were initially made for the performance of these types even though approaching the spherical configuration is optimal for resisting hydrostatic pressure. This is because deeper flexural shells do not have as high a mechanical transformer affect as the shallower versions. This type does not show promise for variable hydrostatic applications.

Cymbal element with holes near the apex did not perform as consistently as expected. Consistent performance started to degrade as hydrostatic pressure approached 500 psi. It is surmised that this type would have better performance in an suitable acoustic field. The inconsistent performance measured at 700 psi is attributed to the fact that other cymbal element types in the test fixture had failed due to hydrostatic stress, thereby allowing air from the cavity to escape, altering the acoustic field and therefore the measured data. Though it is difficult to quantify, air released from these failed units affected the measured performance of the others as well.

Based on the evaluation of previous measurement problems, the acoustic cymbal elements with ports (includes slots and small holes located at the outer edge of the flexural shell) were tested without others that might have failed and introduced a measurement error as presumably had happened earlier with the cymbal element with apex holes. By introducing ports, a conventional and simple method of gaining passive

hydrostatic pressure compensation, the cymbal elements performed reliably and consistently in both the receiving and transmitting modes. The FFVS and TVR both show, within the range of accepted measurement uncertainty in calibrations, a very uniform performance with respect to hydrostatic pressures ranging from ambient pressure to 1250 psi (8619 kPa). Depending on the application, sensitivity and/or transmitting power of these cymbals with ports may need enhancement. However, the consistent behavior of the cymbal elements with ports show they are best suited for Navy sonar systems that must perform with minimal change under a broad spectrum of hydrostatic pressures.

THIS PAGE INTENTIONALLY LEFT BLANK

## LIST OF REFERENCES

1. *Submarine Signal Log*, 1st ed., Raytheon Company, 1953.
2. Hunt, F.V., *ELECTROACOUSTICS, The Analysis of Transduction and its Historical Background*, 2nd ed., pp. 44-45, American Institute of Physics, 1982.
3. Lasky, M., "Review of Undersea Acoustics to 1950," *J. Acoust. Soc. Am.*, v. 61 (20), pp. 283-297, February 1977.
4. Groves, I.D., ed., *Benchmark Papers in Acoustics - Acoustic Transducers*, vol. 15, pp. 258-260, Hutchinson Ross Publishing Company, 1981.
5. Rolt, K.D., "History of the Flexensional Electroacoustic Transducer," *J. Acous. Soc. Am.*, v. 87 (3), pp. 1340-1349, March 1990.
6. Butler, S.C., Butler, A.L., Butler, J.L., "Directional Flexensional Transducer," *J. Acous. Soc. Am.*, 92 (5), pp. 2977-2979, May 1992.
7. Tressler, J.F., Newnham, R.E., "Capped ceramic underwater sound projector: The cymbal transducer," *J. Acous. Soc. Am.*, 105 (2), Pt. 1, February, 1999.
8. McCollum, M.D., Hamonic, B.F., Wilson, O.B., *Transducers for Sonics and Ultrasonics*, pp. 130-131, 141, Technomic Publishing Company, 1992.
9. Meyer Jr., R.J., Dogan, A., Yoon, C., Pilgrim, S.M., Newnham, R.E., "Displacement amplification of electroactive materials using the cymbal flexensional transducer," *Sensors and Actuators*, v. A87, pp. 157-162, July 2000.
10. Personal communication with Professor Robert E. Newnham at The Pennsylvania State University, February 2003.
11. Galassi, C. et al., *Piezoelectric Materials: Advances in Science, Technology and Applications*, pp.357-374, Kluwer Academic Publishers, 2000.
12. Jaffe, B., Cook, W.R., and Jaffe, H., *Piezoelectric Ceramics*, 1st ed., pp. 3, 49-50, Academic Press, 1971.
13. Tressler, J.F., Ph. D. Thesis in Ceramic Science, *Capped Ceramic Underwater Sound Projector: The 'Cymbal'*, August, 1997.
14. Mason, W.P., *Physical Acoustics Principles and Methods, Vol. I, Part A*, pp. 170, 198-200, Academic Press, 1964.

15. Nalwa, H.S., ed., *Handbook of Low and High Dielectric Constant Materials and Their Applications*, vol. 2, pp. 380–383, Academic Press, 1999.
16. Wilson, O.B., *Introduction to the Theory and Design of Sonar Transducers*, 1st ed., U.S. Government Printing Office, Washington, D.C., 1985.
17. Van Renderaat, J. and Settingington, R.E., *Piezoelectric Ceramics*, pp. 4–12, Mullard Limited, 1968.
18. Uchino, K., *Ferroelectric Devices*, pp. 18, 19, 81, Marcel Dekker, Inc., 2000.
19. From University of Waterloo public website, March 2004.  
<http://www.science.uwaterloo.ca/pdf>
20. From University of Missouri-Rolla public website, February 2004.  
[http://web.UMR.edu/~rwschwar/Schwartz\\_Publications/Buchanan%20Figures.pdf](http://web.UMR.edu/~rwschwar/Schwartz_Publications/Buchanan%20Figures.pdf)
21. Bobber, R.J., *Underwater Electroacoustic Measurements*, 2nd ed., pp. 6, 27, 28, 235, 239–240, Peninsula Publishing, 1988.
22. Parker, S.P., ed., *Dictionary of Scientific and Technical Terms*, 3rd ed., p. 395, McGraw-Hill, 1984.
23. Anan'eva, A.A., *Ceramic Acoustic Detectors*, Consultants Bureau, 1965.
24. U.S. Government, *Piezoelectric Ceramic for Sonar Transducers, Military Standard MIL-STD-1376(SHIPS)*, 1970.
25. Naval Research Laboratory Memorandum Report 5687, *Ad Hoc Subcommittee Report on Piezoceramics – Revision of DOD-STD-1376A (SH)*, by A.C. Tims, pp. 1, 6-7, 1 April 1986.
26. Vernitron Piezoelectric Division, *Modern Piezoelectric Ceramics*, Technical Data Brochure PD-9247, 1988.
27. Oberg, E., Jones, F.D., Horton, H.L., *Machinery's Handbook*, 22nd ed., pp. 1929, 2265, Industrial Press Inc., 1984.
28. Clauser, H.R., et al, *The Encyclopedia of Engineering Materials and Processes*, pp. 675-681, Reinhold Publishing, 1963.
29. Althouse, A.D., Turnquist, C.H., Bowditch, W.A., *Modern Welding*, p. 24-23, Goodheart-Willcox Co., 1970.
30. Hewlett Packard, *4194A Impedance/Gain-Phase Analyzer Operations Manual*, pp. 1-1, 1-2, Yokogawa-Hewlett-Packard, Ltd., 1987.



31. Stephens, R.W.B., et al, *International Dictionaries of Science and Technology SOUND*, pp. 30, 253, 408, 423, Halsted Press, 1974.
32. Polytec GmbH, *Operator's Manual for Polytec Scanning Vibrometer PSV-200*, pp. 1-1, 7-2, 7-8, 1997.
33. Howarth, T.R., Tressler, J.F., *A Comparison of Underwater Acoustic Performance of Piezoelectric Ceramic Based Cymbal Projectors*, Oceans 2003 in San Diego, CA, September, 2003.
34. Personal communication with Mr. Tony E. Paolero, measurement facility manager at the Underwater Sound Reference Division, June 2003
35. Based on author's personal knowledge gained from 20 years of experience with moving coil transducers and pressure compensation systems.
36. Personal communication with Dr. Thomas R. Howarth, Naval Sea Systems Command Division Newport, September 2003.
37. Stansfield, D., *Underwater Electroacoustic Transducers*, 1st ed., Bath University Press, 1991.
38. Kinsler, L.E., Frey, A.R., Coppens, Sanders, J.V., *Fundamentals of Acoustics*, 4th ed., John Wiley and Sons, 1982.
39. Butler, J.L., *Underwater Sound Transducers*, Image Acoustics, North Marshfield, MA, 1982.
40. Hanish, S., *A Treatise on Acoustic Radiation, Volume II – Acoustic Transducers*, Naval Research Laboratory, 1983.
41. Urick, R.J., *Principles of Underwater Sound*, 3rd ed., McGraw-Hill, 1983.
42. Crocker, M.J., ed., *Encyclopedia of Acoustics, Volume IV*, p. 1889, John Wiley & Sons, Inc., 1997.

THIS PAGE INTENTIONALLY LEFT BLANK

## APPENDIX A – APTF DATA DIRECTORY 2104

USRD CALIBRATION MEMORANDUM NO. 2104

FEBRUARY 2003

### DATA DIRECTORY

---

#### CHART

##### Cymbal Transducer with Holes at apex

FFVS .....	1-4
Impedance Magnitude .....	5-8
Impedance Phase .....	9-12
TVR .....	13-16

##### Penn State Cymbal Transducer Serial 2DIPR

FFVS .....	17-20
Impedance Magnitude .....	21-24
Impedance Phase .....	25-28
TVR .....	29-32

##### Standard Cymbal Transducer Serial 1

FFVS .....	33-36
Impedance Magnitude .....	37-40
Impedance Phase .....	41-44
TVR .....	45-48

##### Standard Cymbal Transducer Serial 2

FFVS .....	49-52
Impedance Magnitude .....	53-56
Impedance Phase .....	57-60
TVR .....	61-64

##### Standard Cymbal Transducer Serial 3

FFVS .....	65-68
Impedance Magnitude .....	69-72
Impedance Phase .....	73-76
TVR .....	77-80

---

THIS PAGE INTENTIONALLY LEFT BLANK

## APPENDIX B – APTF DATA DIRECTORY 2169

USRD CALIBRATION MEMORANDUM NO. 2169

MAY 2003

### DATA DIRECTORY

---

#### CHART

##### 3mm thick 2dipr #5 Cymbal Element

FFVS .....	1-3
Impedance Magnitude .....	4-6
Impedance Phase .....	7-9
TVR .....	10-12

##### 3mm thick 2dipr #6 Cymbal Element

FFVS .....	13-15
Impedance Magnitude .....	16-18
Impedance Phase .....	19-21
TVR .....	22-24

##### Type 500 with 8mm hole #25 Cymbal Element

FFVS .....	25-26
Impedance Magnitude .....	27-28
Impedance Phase .....	29-30
TVR .....	31-32

##### Type 600 Cymbal Element

FFVS .....	33-34
Impedance Magnitude .....	35-36
Impedance Phase .....	37-38
TVR .....	39-40

##### Type 900 Cymbal Element

FFVS .....	41-42
Impedance Magnitude .....	43-44
Impedance Phase .....	45-46
TVR .....	47-48

---

THIS PAGE INTENTIONALLY LEFT BLANK

## APPENDIX C – APTF DATA DIRECTORY 2228

USRD CALIBRATION MEMORANDUM NO. 2228

AUGUST 2003

### DATA DIRECTORY

---

#### CHART

##### Edge Hole 1 Cymbal Element

FFVS .....	1-3
Impedance Magnitude .....	4-6
Impedance Phase .....	7-9
TVR .....	10-12

##### Edge Hole 2 Cymbal Element

FFVS .....	13-15
Impedance Magnitude .....	16-18
Impedance Phase .....	19-21
TVR .....	22-24

##### Slot 1 Cymbal Element

FFVS .....	25-27
Impedance Magnitude .....	28-30
Impedance Phase .....	31-33
TVR .....	34-36

++679

##### Slot 2 Cymbal Element

FFVS .....	37-39
Impedance Magnitude .....	40-42
Impedance Phase .....	43-45
TVR .....	46-48

---

THIS PAGE INTENTIONALLY LEFT BLANK



## APPENDIX D – TRANSDUCER COORDINATE SYSTEM

UNCLASSIFIED

NAVAL UNDERSEA WARFARE CENTER DIVISION  
UNDERWATER SOUND REFERENCE DETACHMENT  
1176 HOWELL STREET, NEWPORT, RI 02841-1708

(REVISED December 2003 for this report)

### COORDINATE SYSTEM FOR TRANSDUCER OR PANEL ORIENTATION

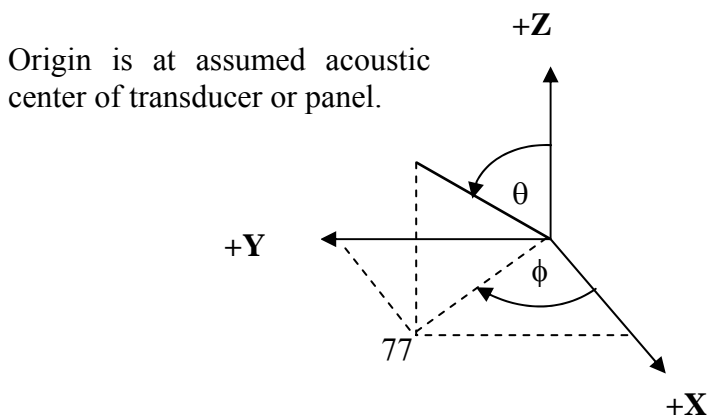
The left-handed coordinate system in the sketch below is affixed to the transducer or panel and moves with it, regardless of its physical position. The angle  $(\theta, \phi)$  denotes the direction of sound propagation. Measurements are made with sound propagated parallel to the positive X axis ( $\theta=90^\circ$ ,  $\phi=0^\circ$ ) unless otherwise specified. For some measurements, the position of an auxiliary transducer may be specified in terms of Cartesian coordinates X, Y, and Z.

Transducers and panels are oriented as follows:

ACOUSTIC SURFACE	ORIENTATION
Cylinder	The cylindrical axis is the Z axis; a reference mark for the +Z direction and for another axis is specified.
Plane	The plane or piston face is the YZ plane, with the X axis normal to the face at the geometric center. A reference mark in the YZ plane is specified.
Sphere	Points on the surface for any two of the three axes are specified.
Other	A sketch of non-conforming configurations is provided.

Directional Response Patterns: Unless otherwise specified, the following apply:

SPECIFIED PLANE	AXIS OF ROTATION	POSITION OF AXES OR DIRECTIONS ON POLAR PLOTS				
		+X AXIS	+Y AXIS	+Z AXIS	$\theta = 45^\circ$ $\phi = 90^\circ$	$\theta = 45^\circ$ $\phi = 270^\circ$
XY	Z	$0^\circ$	$90^\circ$ CW	Upward	-----	-----
XZ	Y	$0^\circ$	Downward	$90^\circ$ CW	-----	-----
YZ	X	Upward	$0^\circ$	$90^\circ$ CW	-----	-----
ROLL	$\theta = 45^\circ$ $\phi = 270^\circ$	$0^\circ$	-----	----- --	$90^\circ$ CW	Upward



THIS PAGE INTENTIONALLY LEFT BLANK

## **INITIAL DISTRIBUTION LIST**

1. Defense Technical Information Center  
Ft. Belvoir, Virginia
2. Dudley Knox Library  
Naval Postgraduate School  
Monterey, California
3. Underwater Sound Reference Division  
Naval Sea Systems Command Division Newport  
Newport, Rhode Island